Nonlinear Dynamics (2026) 114:257
https://doi.org/10.1007/s11071-025-12124-w

RESEARCH

# Effect of fear and refuge in eco-epidemiological model with predator supported by additional food

Raktim Kar[1,2] · Santosh Biswas[1] · A. K. Pal[3] · Juan J. Nieto[4]

Received: 2 September 2025 / Revised: 1 December 2025 / Accepted: 5 December 2025 / Published online: 24 February 2026


**Abstract**
We propose a three-compartment eco-epidemiological model in which prey experience fear from susceptible predators and may seek refuge, predator follows a modified Leslie–Gower growth. The predator population is divided into susceptible and infected class, with disease transmission occurring horizontally together with saturated treatment of infected class. We analyze positivity and boundedness, compute biologically feasible equilibria, and derive the basic reproduction number ($\mathcal{R}_0$) along with conditions for local and global stability. Sensitivity is explored by partial rank correlation coefficient (PRCC) method; bifurcation behaviours are illustrated analytically and numerically. Furthermore, we formulate and numerically solve an optimal control problem aimed at minimizing infected predator biomass and treatment cost using the forward–backward sweep method. The results reveal that larger refuge size and stronger treatment efforts effectively reduce infection prevalence, while fear on prey species control by the refuge. Additionally, the system exhibits parameter-dependent bi-stability and multi-stability, as demonstrated through bifurcation diagrams.

**Keywords** Modified Lesli-Grower eco-epidemiological model · Fear effect · Sensitivity analysis · Bifurcation analysis · Bi-stability · Optimal control

## 1 Introduction

The predator prey interaction has been one of the significant relationship in environment over the past few decades because of its global biological and economic importance. In early stage of the development, predator prey relationship as mathematical modeling quite straightforward and gradually it becomes challenging for researcher. In mathematical modeling, it is crucial to evaluate and validate whether the suggested system will act appropriately within the certain circumstances or not. During the past few decades researchers have done lots of exploration on predator prey system in various biological scenario have extensively studied to anticipate the dynamics of complex system [1–5]. Classical predator prey models, beginning with Malthus [6] and later extended by Lotka [7] and Voltera [8], from the foundation of predator prey theory. Modern studies have since incorporated additional ecological complexities such as fear [1, 9], refuge [10], and infection [4] to describe realistic predator prey dynamics.

From the pioneering study of Anderson and May [11], many researchers have examined eco-epidemiological system incorporating infection in prey [4, 12–17] or predator [10, 18–21] and both [22]. The studies revealing diversified behavioral phenomenon such as oscillation, bi-stability and thresholds of the extinction depending on the disease transmission. Zhi et al. [23] established that the transmission rate of a virus and the recovery rate of hosts is affected by human intervention providing a clue to reduce the infection rate and

✉ Juan J. Nieto
juanjose.nieto.roig@usc.es

Raktim Kar
raktimkarmathematics@gmail.com

Santosh Biswas
sant_biswas@yahoo.in

A. K. Pal
akpal_2002@yahoo.co.in

1 Centre for Mathematical Biology and Ecology, Department of Mathematics, Jadavpur University, 188, Raja S. C. Mallik Road, Kolkata, West Bengal 700032, India

2 Department of Mathematics, Brainware University, 398, Ramkrishnapur Road, Barasat, Kolkata 700125, India

3 Department of Mathematics, Seth Anandram Jaipuria College, 10, Raja Nabakrishna Street, Kolkata 700005, India

4 CITMAga, Universidade de Santiago de Compostela, Santiago de Compostela 15782, Spain

mitigating the harm caused by the virus. Recently in ecological system, effect of fear plays a significant role among the various ecological phenomena. The predation effect can change the ecology of prey species directly and indirectly based on the behavioral aspects of predator species. Not only the direct impact of mortality but also fear of predation, affect the demography and life style of entire prey population [24]. Suraci et al. [25] mentioned in their work, predation fear exerts significant impact in changing the prey vigilance behavior. Several researchers [26–29] demonstrated in their work that incorporating fear effect into the prey species can reduce the reproduction rate, potentially leading to decline population density or even extinction under certain condition. Researchers are explored the predator prey modeling works inducting the effect of fear in predator–prey ecological system dynamics [30–32]. Researchers are also explored the eco-epidemiological system [10, 18, 20], time delay system [33], fractional order model with fear effect [34]. Wang et al. [27] first mentioned the fear function in the Rosenzweig-MacArthur predator–prey model [35]. The authors [27] established in their work, fear may stabilize predator prey dynamics by remove the existence of limit cycle oscillation and in the effect of fear system showed supercritical as well as subcritical Hopf bifurcation. Sha et al. [18] demonstrated in their work high value of fear due to the predation and the disease transmission stabilized the system. Along with that system exhibits trancritical and Hopf bifurcation with respect to the disease transmission rate for different values of fear effect. Panday et al. [33] showed that fear induced delay is stabilized or destabilized effects, which is depending on the magnitude of the delay parameter. Notably, gradually increment of magnitude of delay system showed switching phenomena in between stable focus and oscillatory limit cycle. On the other hand higher value of delay, the system experienced chaotic regime. Mandal et al. [34] showed that higher value of fear maintain stable nature but the lower value exhibits oscillatory nature result through occurrence of Hopf bifurcation. The chaotic oscillation eliminated from an eco-epidemiological model due to the predation of fear mentioned by Pal [20]. Barman et al. [30] described that high strength of predation fear in two species predator–prey model destabilized the system.

In environment, it's quite common phenomena for predator species hunting the prey species for survive. However it's also true that predator species can't capture total prey population due to the effect of predation, psychologically developed a anti-predator behavior in prey species. The result of this, prey population seeking refuge to evade the predation risk [36]. This signify that refuge attitude in prey species protect from the high predation. This refuge attitude playing the vital role in predator–prey interaction. Recently researchers are considered their work prey refuge as a vital component of predator–prey model due to realistic biological scenario [10, 37]. Moreover most of the researcher are consider direct predation in predator–prey system is the only way to killed the prey population, but which deffer from the real world scenario, where prey alter their behavior due to the presence of predator species [27, 38]. The prey populations are gradually developing the anti-predator behavior due to the predation risk, including vigilance, adjusting foraging and internal changes. This changes are reduce short term predation risk, which effects significantly on the reproduction rate in long term [39].

Generally the researchers are considered that the predator species consuming prey species and convert it in energy, is the only factor to sustain for predator growth. Nevertheless, there are multiple features to influence the persistence of the predator species in long term effect. In 1948 Leslie [40] proposed in his work the predator species can't grow limitlessly, subject to the limitations of natural environment. The predator population will stabilized, when the prey population grows with in a stipulated range. The growth of prey species is not shaped in a constant rate, due to the diversified growth of prey species. The classical Leslie-Gower predator prey model [41], the carrying capacity plays a pivotal role in regulating the dynamics potentially inconsistency in predator species. The growth rate of predator species mathematically in a form $\frac{dp}{dt} = r_2 p\left(1 - \frac{p}{\delta n}\right)$, where $r_2$ growth rate of predator species $p$ and $\delta$ is the conversion factor of prey $(n)$ into predator and the term $\frac{p}{\delta n}$ is denoted as Leslie-Gower term. Nonetheless, numerous predator exist in the environment they do not live just one kind of food. In the absence of their favorite food, then the predator species move to capture the other prey species for survival. Therefore the predators environmental carrying capacity doesn't adequately explain this biological phenomenon. After that Aziz-Alaou and Okiye [42] constructed a modified Leslie-Gower predator prey model, the modified model quite precisely replicate the relationship between predator and prey. The modified model reflect that the predator species live due the presence of alternating prey. The modified model represented as $\frac{dp}{dt} = r_2 p\left(1 - \frac{p}{\delta n + k}\right)$, where the additional term $k$ represent the alternating food source. Recently [20, 31] considered in their work modified Leslie-Gower functional response and showed that, the predator species not goes to extinction due to the presence of alternating food resources. Along with that, the effect of predation psychologically developed a anti predator behavior in prey species which leads to the refuge like phenomena. To the based on that phenomena Vinoth et al. [37] considered the refuge due to the predation risk, and the rate of change of predator species represented as $\frac{dp}{dt} = r_2 p\left(1 - \frac{p}{\delta n(1-\mu p)+k}\right)$, where $\mu np$ is the refuge size from the predator species.

### 1.1 Motivation and novelty of the research

To the best of our knowledge, very few researchers are work on treatment function in eco-epidemiological system. They did not considered the treatment function for an eco-epidemiological system where infection in predator. Moreover there are very few researchers considered fear [3] and refuge together in their work [43, 44] but no one is considered disease in predator species. Mondal et al. [10] considered in their work predation fear, prey refuge together in prey species and infection in predator along with that treatment for infected predator species but they do not considered alternating food resources for predator species to prevent them from extinction. To address this gap, we propose a novel eco-epidemiological model that combines multiple realistic epidemiological factors rarely examined together. The key novelties of this work are

- We incorporate fear-induced behavioural modification in prey along with a proportional prey refuge, capturing both non-consumptive and protective responses to predation risk.
- The predator population follows a modified Leslie—Gower growth structure that includes additional food resources, allowing the predator to persist even when prey density is very low or in extinction.
- The model introduces a realistic saturating treatment term for infected predators, reflecting limited medical resources and treatment delay.
- PRCC-based sensitivity analysis identifies the most influential parameters which helps to increase the infection. Through the violin diagram provides a comprehensive visualization of the distribution and reliability of PRCC values through bootstrapped simulations.
- An optimal control framework is developed to minimize infection with cost-effective treatment strategies. Numerical simulations reveal that the interplay of fear, refuge, disease transmission, and treatment can induce bi-stability and multi-stability, providing rich dynamical behavior and insights into ecological resilience.

Overall, this work provides an integrated theoretical framework linking ecological fear effects, refuge behaviour, disease transmission, and treatment strategies, offering novel insights into sustaining predator populations and managing infection in eco-epidemiological systems.

### 1.2 Structure of the manuscript

This manuscript is organized as follows. The model formulation is presented in Sect. 2. Positivity and boundedness is discussed in Sect. 3. Section 4 illustrates all the biologically feasible equilibrium points and the basic reproduction number. Section 5 describes the local stability. Section 6, we analyze the global stability around the equilibrium points. Bifurcation analysis of the model described in Sect. 7. Section 8 contains sensitivity analysis using PRCC technique. Section 9 deals with normalized sensitivity analysis of reproduction number. Section 10 describes the optimal control strategy. Numerical simulation is given for validation of our theoretical analysis in Sect. 11. Finally, the paper ends with discussion and conclusion of this work in Sect. 12.

## 2 Model formulation

In this article, we consider a predator–prey eco-epidemiological model where the prey population grows at a rate ($r_1$) in the absence of predators and fear of predation. The predator population carries the disease and the prey species transit to the decline zone due to fear of predation induced by the susceptible predator. Let $n(t)$ represents the number of prey species at time $t$, while the predators are divided into two compartment: susceptible predator $p_s(t)$ and infected predator $p_i(t)$ at time $(t)$.

The prey species grows logistically in the absence of predator, and the growth is influenced by intra species competition ($\nu$) and natural death rate ($d_1$). The fear induced by the susceptible predator has a negative impact on the reproduction of prey species [29]. To capture this influence, we introduce a function $\Pi(f, p_s)$ that modifies the growth rate on prey, where $f$ represents the effect of fear due to the presence of susceptible predator. So we can express the scenario in the form of first order ordinary differential equation

$$\frac{dn}{dt} = r_1 n \Pi(f, p_s) - d_1 n - \nu n^2,$$

where $\Pi(f, p_s) = \frac{1}{1+fp_s}$, which is denoted as fear function and follows the conditions:

- $\Pi(0, p_s) = \Pi(f, 0) = 1$, it implies that the growth rate of the prey population remains unaffected in the absence of healthy predators or fear effects.
- $\lim_{f\to\infty} \Pi(f, p_s) = \lim_{p_s\to\infty} \Pi(f, p_s) = 0$, which implies that an increase the fear level or the density of susceptible predators leads to a reduction in the prey's growth rate, which may completely vanish when the fear effect is sufficiently high.
- $\frac{\partial \Pi(f,p_s)}{\partial f} < 0$ and $\frac{\partial \Pi(f,p_s)}{\partial p_s} < 0$, which implies that growth of prey population decreases with an increase of fear level and the boost of predator abundance.

The combined effect of predation and fear of predation lead to a reduction the biomass or may even drive the population towards extinction [20]. To provide protection against

predation, we incorporate proportional prey refuge denoted by $m$ [37]. The susceptible predator species consumed prey species according to the Holling type-II functional response at a rate ($\alpha$) and infected predator consumed prey species in a lower rate $\alpha g$ where ($0 < g < 1$) denotes the reduction factor in the predation efficiency due to weakness caused by infection [10]. Hence the rate of change of the prey species is expressed by the following ODE:

$$\frac{dn}{dt} = \frac{r_1 n}{1 + f p_s} - d_1 n - \nu n^2 - \frac{\alpha(1-m)n}{a + (1-m)n}(p_s + g p_i).$$

Here $a$ is half saturation constant.

Infected predators are too weak to induce fear in the prey species. due to the weakness. Thus only susceptible predator exert a meaningful impact on the growth of prey population. Such an effect classify the favorite food of susceptible predators may not always be available in sufficient quantity [20]. Consequently, the predator species are moving to alternative food sources, as discussed by Aziz-Alaou and Okiye [42], leading to formulation of the modified Leslie-Gower predator prey model. To preserve the environmental as well as ecological sustainability, we consider the modified Leslie-Gower response in modeling the growth of susceptible predator species at a rate of ($r_2$). Furthermore, the susceptible predators are negatively affected by the infected predator due to horizontal interactions between the two predator classes occurring at the rate of ($e$). In addition, we incorporate a saturating treatment function following [45, 46], characterized by the treatment rate ($\gamma$) and the treatment delay ($\beta$), to capture the realistic limitations of medical or ecological recovery processes. In natural ecosystems, the recovery of infected individuals cannot increase indefinitely with infection intensity because of resource constraints, delayed responses to treatment, or other biological restrictions. The inclusion of ($\beta$) accounts for the time lag between disease detection and effective treatment, while ($\gamma$) determines the maximum medical resource supplied for treatment. This formulation ensures that the transition of infected predators back to the susceptible class occurs at a biologically feasible rate, thereby enhancing susceptible predator density and contributing to the long-term stability and ecological balance of the system. Introducing this phenomenon the rate of change of susceptible predator represents as

$$\frac{dp_s}{dt} = p_s\left\{r_2\left(1 - \frac{p_s}{\eta + (1-m)n}\right) - e p_i - d_2\right\} + \frac{\gamma p_i}{\beta + p_i}.$$

where $d_2$ is the death rate of susceptible predator and $\beta$ is the delay of treatment.

In our model, the infected predator population increases solely through the transmission process from the susceptible predators. The infected predators are too weak to consume prey effectively; hence, prey consumption does not significantly contribute to their growth. This implies that the growth of the infected predator population depends entirely on the abundance of susceptible predators [10, 20]. Additionally, we incorporate a treatment function aimed at reducing the infected predator population and promoting the recovery of individuals to the healthy (susceptible) class, thereby enhancing the overall predator biomass [10]. Accordingly, the growth rate of the infected predator population can be expressed in the model by the following differential equation:

$$\frac{dp_i}{dt} = p_i\left\{e p_s - d_3 - \frac{\gamma}{\beta + p_i}\right\}.$$

Here $d_3$ represents the death rate of infected predator.

Based on the above assumptions we have the following eco-epidemiological model with infection present in predator species.

$$\begin{aligned}
\frac{dn}{dt} &= \frac{r_1 n}{1 + f p_s} - d_1 n - \nu n^2 - \frac{\alpha(1-m)n}{a + (1-m)n}(p_s + g p_i),\\
\frac{dp_s}{dt} &= p_s\left\{r_2\left(1 - \frac{p_s}{\eta + (1-m)n}\right) - e p_i - d_2\right\} + \frac{\gamma p_i}{\beta + p_i},\\
\frac{dp_i}{dt} &= p_i\left\{e p_s - d_3 - \frac{\gamma}{\beta + p_i}\right\}.
\end{aligned} \tag{1}$$

For clear understanding, we also prescribe biological interpretation of each term in system (1) is as follows:

$$\begin{aligned}
\frac{dn}{dt} = {} & \underbrace{\frac{r_1 n}{1 + f p_s}}_{\substack{\text{Prey's growth reduced}\\ \text{by fear } (f) \text{ induced by}\\ \text{susceptible predators}}} - \underbrace{d_1 n}_{\text{natural mortality}} - \underbrace{\nu n^2}_{\text{intra-species competition}}\\
& - \underbrace{\frac{\alpha(1-m)n(p_s + g p_i)}{a + (1-m)n}}_{\substack{\text{Holling type-II predation reduced}\\ \text{by refuge } m,\ \text{infected feed at rate } g\in(0,1)}},\\
\frac{dp_s}{dt} = {} & \underbrace{r_2 p_s\left(1 - \frac{p_s}{\eta + (1-m)n}\right)}_{\substack{\text{Leslie-Gower growth with}\\ \text{alternative food source } \eta}} - \underbrace{e p_s p_i}_{\text{horizontal disease transmission}}\\
& - \underbrace{d_2 p_s}_{\text{susceptible mortality}} + \underbrace{\frac{\gamma p_i}{\beta + p_i}}_{\substack{\text{saturating treatment moving}\\ \text{infected to susceptible class}}},\\
\frac{dp_i}{dt} = {} & \underbrace{e p_s p_i}_{\text{infection growth}} - \underbrace{d_3 p_i}_{\text{infected mortality}} - \underbrace{\frac{\gamma p_i}{\beta + p_i}}_{\text{removal by treatment}}.
\end{aligned}$$

The biological meaning of all the parameters and their numerical values used in the above model (1) is mentioned in the Table 1. We analyze model (1) by considering positive initial values of the state variables, i.e., $n(0) = n_0 > 0$, $p_s(0) = p_{s_0} > 0$ and $p_i(0) = p_{i_0} > 0$.

The proposed system (1) includes 15 parameters, which allows to capture complex eco-epidemiological interactions. However, accurately assessing all parameters from real world data can be challenging, and full identifiability may not always be achievable. In this study, parameter values were chosen depended on biologically realistic estimates from the literature or analytical assumptions, and sensitivity analysis was executed to identify the parameters that most strongly influence system (1) dynamics.

## 3 Positivity and boundedness

**Theorem 1** *Solution of the system (1) with the positive initial condition remain non negative every time for $t \geq 0$.*

***Proof*** The right hand side of the system (1) is a continuous functions of dependent variables, after integrating the first equation of (1). From the first equation of our system (1) we get,

$$n(t) = n(0)\exp\left(\int_0^t \left[\frac{r_1}{1+fp_s(\tau)} - d_1 - \nu n(\tau) - \frac{\alpha(1-m)}{a+(1-m)n(\tau)}(p_s(\tau)+gp_i(\tau))\right]d\tau\right)$$

and satisfies $n(t) > 0$ for all $t > 0$.

For the third equation of the system (1) we get,

$$p_i(t) = p_i(0)\exp\left(\int_0^t \left[ep_s(\tau) - d_3 - \frac{\gamma}{\beta + p_i(\tau)}\right]d\tau\right)$$

and satisfies $p_i(t) > 0$ for all $t > 0$.

To prove the positivity of $p_s(t)$ for $t \in [0, \infty)$ we consider the process as follows. Let us assume there exist a $t^* > 0$, such that $p_s(t^*) = 0$, $\frac{dp_s}{dt} < 0$ and $p_s(t) > 0$. Therefore from the second equation of the system (1) we get,

$$\frac{dp_s(t)}{dt} \geq p_s(0)\exp\left(\int_0^t \left[r\left(1 - \frac{p_s(\tau)}{\eta + (1-m)n(\tau)}\right) - ep_i(\tau) - d_2\right]d\tau\right).$$

which contradicts our assumption $\frac{dp_s}{dt} < 0$. Hence $p_s(t) \geq 0$ for all $t \geq 0$. Therefore, the system (1) with the positive initial condition are always non-negative. □

**Theorem 2** *All the solution of the system (1) with positive initial values begin with $\mathbb{R}^3_+$ are uniformly bounded.*

***Proof*** Let $L = n + p_s + p_i$, then

$$\begin{aligned}\frac{dL}{dt} &= \frac{dn}{dt} + \frac{dp_s}{dt} + \frac{dp_i}{dt}\\ &\leq \frac{r_1 n}{1+fp_s} - d_1 n - \nu n^2 + p_s\left\{r_2\left(1 - \frac{p_s}{\eta + (1-m)n}\right) - d_2\right\} - d_3 p_i\\ &\leq (r_1 n - \nu n^2) - d_1 n + \left(p_s r_2 - \frac{r_2 p_s^2}{\eta + (1-m)n}\right) - d_2 p_s - p_i d_3\\ &\leq \frac{r_1^2}{4\nu} + \frac{r_2 k}{4} - \rho L. \text{ [considering } k = \eta + (1-m)\frac{r_1^2}{4\nu}\text{ ].}\end{aligned}$$

where, $\frac{r_1^2}{4\nu}$ and $\frac{r_2 k}{4}$ are the maximum values of $r_1 n - \nu n^2$ and $p_s r_2 - \frac{r_2 p_s^2}{\eta+(1-m)n}$ respectively. Thus, $\frac{dL}{dt} \leq \frac{r_1^2}{4\nu} + \frac{r_2 k}{4} - L\rho$, where $\rho = min\{d_1, d_2, d_3\}$. For $t \to \infty$ we have $0 < L \leq \frac{G}{\rho}$, where $G = \frac{r_1^2}{4\nu} + \frac{r_2 k}{4}$. Hence, all the solution of the system (1) enter into the region

$$B = \{(n, p_s, p_i) \in \mathbb{R}^3_+ : 0 < L \leq \frac{G}{\rho} + \epsilon\}$$

for any $\epsilon > 0$ and for $t \to \infty$. □

## 4 Equilibrium points and basic reproduction number of the system (1)

In this section, we discuss the existence of biologically feasible equilibrium points of model system (1) and hence we calculate the basic reproduction number of the model by next-generation matrix method.

### 4.1 Equilibrium points

In order to obtain different equilibrium points of the system (1), we set $\frac{dn}{dt} = \frac{dp_s}{dt} = \frac{dp_i}{dt} = 0$. By doing so, we get following non-negative equilibria of the system (1):

1. The predator-free equilibrium point (PFEP) $E_1 = \left(\frac{r_1 - d_1}{\nu}, 0, 0\right)$, exists when $r_1 > d_1$.
2. The prey and disease free equilibrium point (PDFEP) $E_2 = \left(0, \frac{(r_2 - d_2)\eta}{r_2}, 0,\right)$ exists when $r_2 > d_2$.
3. The infection-free equilibrium point (IFEP) $E_3 = (\bar{n}, \bar{p_s}, 0)$, where $\bar{n} = \left(\frac{\bar{p_s} - k\eta}{k(1-m)}\right)$, $k = \left(\frac{r_2 - d_2}{r_2}\right)$ and $\bar{p_s} > 0$ satisfy the equation:

$$A_1 \bar{p_s}^3 + 3A_2 \bar{p_s}^2 + 3A_3 \bar{p_s} + A_4 = 0. \quad (2)$$

where,

$$A_1 = \nu f,$$
$$3A_2 = \nu(1 + afk) + fk\left\{\alpha k(1-m)^2 - d_1(1-m) - 2\nu\eta\right\},$$

**Table 1** Descriptions of parameters in system (1)

| Parameters | Biological description | Numerical value |
|---|---|---|
| $r_1$ | Growth rate of prey species | 2.0 [30] |
| $f$ | Fear effect on reproduction of prey due to the presence of susceptible predator | 0.2 [31] |
| $d_1$ | Natural death rate of the prey species | 0.015 [32] |
| $\nu$ | Intra-species competition | 0.15 [10] |
| $\alpha$ | Consumption rate | 0.25 [10] |
| $m$ | Proportion of prey refuge | 0.2 [10] |
| $a$ | Half saturation constant | 0.7 [10] |
| $g$ | Reduction factor in the predation efficiency of infected predator, lies between 0 and 1 (dimensionless) | 0.05 |
| $r_2$ | Growth rate of predator species | 0.4 [20] |
| $\eta$ | Alternating food source | 1.9 |
| $e$ | Disease transmission rate | 0.41 [10] |
| $d_2$ | Natural death rate of susceptible predator | 0.011 [10] |
| $\gamma$ | Maximum medical resource supplied for treatment | 0.5 [10] |
| $\beta$ | Saturation factor measuring the effect of delayed treatment | 0.7 |
| $d_3$ | Death rate of infected predator | 0.7 |

$$
\begin{aligned}
3A_3 &= d_1k^2(1-m)(a-\eta)f + \nu ak + \nu fk^2\eta^2 + \alpha k^2(1-m)^2 \\
&\quad -(r_1-d_1)(1-m)k - 2\nu\eta k - \nu fa\eta k^2, \\
A_4 &= \{(r_1-d_1)(1-m)+\nu\eta\}k^2(\eta-a).
\end{aligned}
$$

The above equation (2) has exactly one real positive root if $\kappa + 4\tau^3 > 0$, where $\kappa = A_1^2A_4 - 3A_1A_2A_3 + 2A_2^3$ and $\tau = A_1A_3 - A_2^2$. If $\omega$ denotes one of the cubic roots of $\frac{1}{2}[-\kappa+\sqrt{\kappa+4\tau^3}]$, then by Cardano's method, the root is given by $\frac{1}{A_1}[\omega - A_2 - \frac{\tau}{\omega}]$. When $\kappa+4\tau^3 = 0$, equation (2) has two equal roots, whereas the condition $\kappa + 4\tau^3 < 0$ together with $\tau < 0$ yields three distinct real roots. Here, $E_3$ denotes the unique positive infection-free equilibrium point of the system (1); however, when equation (2) admits three distinct positive roots, the system can possess three different infection free equilibrium points.

4. The interior equilibrium point (IEP) $E^* = (n^*, p_s^*, p_i^*)$, where $n^*$, $p_s^*$, $p_i^*$ are the positive roots of the following set of equations:

$$\frac{r_1}{1+fp_s^*} - d_1 - \nu n^* - \frac{\alpha(1-m)}{a+(1-m)n^*}(p_s^* + gp_i^*) = 0, \tag{i}$$

$$p_s^*\left\{r_2\left(1-\frac{p_s^*}{\eta+(1-m)n^*}\right) - ep_i^* - d_2\right\} + \frac{\gamma p_i^*}{\beta+p_i^*} = 0, \tag{ii}$$

$$ep_s^* - d_3 - \frac{\gamma}{\beta+p_i^*} = 0. \tag{iii}$$

From equation (iii), we obtain

$$p_s^* = \frac{1}{e}\left(d_3 + \frac{\gamma}{\beta+p_i^*}\right). \tag{3}$$

Substituting $p_s^*$ into equation (ii), the expression for $n^*$ in terms of $p_i^*$ is obtained as

$$n^* = \frac{1}{(1-m)}\left[\frac{r_2\left(p_s^*\right)^2}{r_2p_s^* - p_s^*(ep_i^* + d_2) + \dfrac{\gamma p_i^*}{\beta+p_i^*}} - \eta\right], \tag{4}$$

where $p_s^*$ is given by (3). Finally, substituting $p_s^*$ from (3) and $n^*$ from (4) into equation (i), we obtain a single equation in $p_i^*$ of the form

$$
\begin{aligned}
F(p_i^*) &= \frac{r_1}{1+f\,p_s^*(p_i^*)} - d_1 - \nu\, n^*(p_i^*) \\
&\quad - \frac{\alpha(1-m)}{a+(1-m)n^*(p_i^*)}\left(p_s^*(p_i^*) + gp_i^*\right) = 0,
\end{aligned} \tag{5}
$$

where $F(p_i^*) = 0$ determines the equilibrium value(s) of the infected predator population $p_i^*$. The corresponding positive equilibria $(n^*, p_s^*, p_i^*)$ are obtained by substituting each positive root of (5) into (3) and (4). Since, it is analytically quite difficult to determine the number of positive root from the equation (5), we calculate it numerically for $p_i^*$. The corresponding values of $p_s^*$ and $n^*$ are then evaluated from (3) and (4) respectively, under the condition $\left\{r_2\left(p_s^*\right)^2 + \eta p_s^*(ep_i^* + d_2)(\beta + p_i^*)\right\} > \eta\left\{p_s^*(\beta+p_i^*)r_2 + \gamma p_i^*\right\}$.

### 4.2 Basic reproduction number ($\mathcal{R}_0$)

The basic reproduction number $\mathcal{R}_0$ indeed represents the average number of new infections generated by an infected species in a completely susceptible environment. This captures the ability of the virus to spread within the population of uninfected species. According to [10, 22, 47], the basic reproduction number $\mathcal{R}_0$ in eco epidemiological model system (1) can be obtained by using next-generation matrix method. The next generation matrix method is applied here due to the disease transmission in our system (1) is restricted to predator compartments and the equations can be decomposed into new infection terms and transition terms as required by the next generation matrix framework. In our model system, we have

$$F = (e\bar{p_s})_{1\times 1} \quad \text{and} \quad V = \left(d_3 + \frac{\gamma}{\beta}\right)_{1\times 1}.$$

Therefore the next generation matrix:

$$FV^{-1} = \left(\frac{e\beta\bar{p_s}}{\beta d_3 + \gamma}\right)_{1\times 1}.$$

$\mathcal{R}_0 = \rho(FV^{-1})$, where $\rho$ denotes the spectral radius, i.e., largest eigenvalue of the matrix $FV^{-1}$. Thus $\mathcal{R}_0 = \frac{e\beta\bar{p_s}}{\beta d_3+\gamma}$.

## 5 Local stability analysis

In this section we analyze the local stability of the system (1) around the obtained equilibrium pints. To do this, we compute the Jacobian matrix of the system (1) at a general equilibrium point $E = (n, p_s, p_i)$ and is given by:

$$J(E) = \begin{pmatrix} u_{11} & u_{12} & u_{13} \\ u_{21} & u_{22} & u_{23} \\ u_{31} & u_{32} & u_{33} \end{pmatrix},$$

where

$$u_{11} = \frac{r_1}{1+fp_s} - d_1 - \nu n - \frac{\alpha(1-m)}{a+(1-m)n}(p_s + gp_i) + n\left(-\nu + \frac{\alpha(1-m)^2(p_s+gp_i)}{(a+(1-m)n)^2}\right),$$

$$u_{12} = n\left\{-\frac{r_1 f}{(1+fp_s)^2} - \frac{\alpha(1-m)}{a+n(1-m)}\right\},$$

$$u_{13} = -\frac{\alpha g(1-m)n}{a+n(1-m)},\ u_{21} = \frac{r_2(1-m)p_s^2}{(\eta+(1-m)n)^2},$$

$$u_{22} = \left\{r_2\left(1 - \frac{p_s}{\eta+(1-m)n}\right) - ep_i - d_2\right\} - \frac{r_2 p_s}{\eta+(1-m)n},$$

$$u_{23} = -ep_s + \frac{\beta\gamma}{(\beta+p_i)^2},$$

$$u_{31} = 0,\ u_{32} = ep_i,\ u_{33} = \left\{ep_s - d_3 - \frac{\gamma}{\beta+p_i}\right\} + \frac{p_i\gamma}{(\beta+p_i)^2}.$$

We summarize the qualitative nature of the system (1) around different equilibrium points in the following theorem.

**Theorem 3** *1. The predator-free equilibrium point $E_1$ is stable provided $r_2 < d_2$.*

2. *The equilibrium point $E_2$ is stable, if the equilibrium point exist along with the conditions $\frac{r_1 r_2}{r_2+f(r_2-d_2)\eta} < d_1 + \frac{\alpha(1-m)(r_2-d_2)\eta}{ar_2}$ and $\frac{e(r_2-d_2)\eta}{r_2} < d_3 + \frac{\gamma}{\beta}$ hold.*
3. *The equilibrium point $E_3$ is stable, if $\mathcal{R}_0 < 1$, $u_{11}^{[3]} + u_{22}^{[3]} < 0$ and $u_{11}^{[3]}u_{22}^{[3]} - u_{12}^{[3]}u_{21}^{[3]} > 0$.*
4. *The interior equilibrium $E^*$ is locally asymptotically stable if and only if following conditions are satisfied.*

$$(i)\ n^*\nu + 2\frac{r_2 p_s^*}{\eta+(1-m)n^*} + ep_i^* + d_2 > r_2 + \frac{\alpha(1-m)^2(p_s^* + gp_i^*)}{(a+(1-m)n^*)^2} + \frac{\gamma p_i^*}{(\beta+p_i^*)^2},$$

$$(ii)\ u_{12}^*u_{21}^* > u_{11}^*u_{22}^* \quad and \quad u_{11}^*u_{23}^* > u_{13}^*u_{21}^*,$$

$$(iii)\ u_{13}^*u_{21}^*u_{32}^* + u_{12}^*u_{21}^*(u_{11}^* + u_{22}^*) > u_{33}^*(u_{11}^* + u_{22}^*)^2 + (u_{11}^*u_{22}^* + {u_{33}^*}^2)(u_{11}^* + u_{22}^*).$$

***Proof*** 1. The Jacobian matrix at the boundary equilibrium point $E_1$ is given by

$$J(E_1) = \begin{pmatrix} -(r_1-d_1) & -\frac{(r_1-d_1)}{\nu}\left(r_1 f\nu + \frac{\alpha\nu(1-m)}{a\nu+(1-m)(r_1-d_1)}\right) & -\frac{\alpha g(1-m)(r_1-d_1)}{a\nu+(r_1-d_1)(1-m)} \\ 0 & r_2 - d_2 & \frac{\gamma}{\beta} \\ 0 & 0 & -d_3 - \frac{\gamma}{\beta} \end{pmatrix}.$$

The eigenvalues of above matrix are $-(r_1-d_1)$, $r_2-d_2$ and $-d_3 - \frac{\gamma}{\beta}$. Hence, the system (1) is stable at the equilibrium point $E_1$ if $r_2 < d_2$.

2. The Jacobian matrix at the boundary equilibrium point $E_2$ is given by

$$J(E_2) = \begin{pmatrix} \frac{r_1 r_2}{r_2 + f(r_2-d_2)\eta} - d_1 - \frac{\alpha(1-m)(r_2-d_2)\eta}{ar_2} & 0 & 0 \\ \frac{(r_2-d_2)^2}{r_2}(1-m) & -(r_2-d_2) & -e\frac{(r_2-d_2)\eta}{r_2} + \frac{\gamma}{\beta} \\ 0 & 0 & e\frac{(r_2-d_2)\eta}{r_2} - d_3 - \frac{\gamma}{\beta} \end{pmatrix}.$$

The eigenvalues of above matrix are $\frac{r_1 r_2}{r_2 + f(r_2-d_2)\eta} - d_1 - \frac{\alpha(1-m)(r_2-d_2)\eta}{ar_2}$, $-(r_2-d_2)$ and $e\frac{(r_2-d_2)\eta}{r_2} - d_3 - \frac{\gamma}{\beta}$. Hence, the system (1) is stable at the equilibrium point $E_2$ if $\frac{r_1 r_2}{r_2 + f(r_2-d_2)\eta} < d_1 + \frac{\alpha(1-m)(r_2-d_2)\eta}{ar_2}$ and $\frac{e(r_2-d_2)\eta}{r_2} < d_3 + \frac{\gamma}{\beta}$.

3. The Jacobian matrix of the system (1) at the equilibrium $E_3$ is given by

$$J(E_3) = \begin{pmatrix} u_{11}^{[3]} & u_{12}^{[3]} & u_{13}^{[3]} \\ u_{21}^{[3]} & u_{22}^{[3]} & u_{23}^{[3]} \\ 0 & 0 & u_{33}^{[3]} \end{pmatrix},$$

where

$$\begin{aligned} u_{11}^{[3]} &= \bar{n}\left(-\nu + \frac{\alpha(1-m)^2\bar{p}_s}{(a+(1-m)\bar{n})^2}\right), \\ u_{12}^{[3]} &= \bar{n}\left\{-\frac{r_1 f}{(1+f\bar{p}_s)^2} - \frac{\alpha(1-m)}{a+\bar{n}(1-m)}\right\}, \\ u_{13}^{[3]} &= -\frac{\alpha g(1-m)\bar{n}}{a+\bar{n}(1-m)}, \\ u_{21}^{[3]} &= \frac{r_2(1-m)\bar{p}_s{}^2}{(\eta+(1-m)\bar{n})^2}, \\ u_{22}^{[3]} &= (r_2-d_2) - \frac{2r_2\bar{p}_s}{\eta+(1-m)\bar{n}}, \\ u_{23}^{[3]} &= -e\bar{p}_s + \frac{\gamma}{\beta}, u_{33}^{[3]} = e\bar{p}_s - \frac{\gamma}{\beta} - d_3. \end{aligned}$$

The characteristic equation associated with the above matrix is given by

$$(u_{33}^{[3]} - \lambda)\left\{\lambda^2 - (u_{11}^{[3]} + u_{22}^{[3]})\lambda + (u_{11}^{[3]}u_{22}^{[3]} - u_{12}^{[3]}u_{21}^{[3]})\right\} = 0. \tag{6}$$

Clearly, one eigenvalue is $u_{33}^{[3]}$, which is negative if $\mathcal{R}_0 < 1$. The other two eigenvalues are negative or have negative real parts provided $u_{11}^{[3]} + u_{22}^{[3]} < 0$ and $u_{11}^{[3]}u_{22}^{[3]} - u_{12}^{[3]}u_{21}^{[3]} > 0$. Therefore we get all the eigenvalues of the characteristic equation are negative or have negative real parts if the conditions stated in the theorem are satisfied. Thus, the disease-free equilibrium $E_3$ is locally asymptotically stable.

*Remark.* The sufficient conditions for infection free equilibrium point (IFEP) $E_3$ is locally asymptotically stable when $\mathcal{R}_0 < 1$, $u_{11}^{[3]} < 0$ and $u_{22}^{[3]} < 0$.

4. Entries of the Jacobian matrix $J(E^*) = (u_{ij}^*)_{3\times 3}$ at the equilibrium point $E^*$ are

$$\begin{aligned} u_{11}^* &= n^*\left(-\nu + \frac{\alpha(1-m)^2(p_s^* + gp_i^*)}{(a+(1-m)n^*)^2}\right), \\ u_{12}^* &= n^*\left\{-\frac{r_1 f}{(1+fp_s^*)^2} - \frac{\alpha(1-m)}{a+n^*(1-m)}\right\}, \\ u_{13}^* &= -\frac{\alpha g(1-m)n^*}{a+n^*(1-m)},\ u_{21}^* = \frac{r_2(1-m)p_s^{*2}}{(\eta+(1-m)n^*)^2}, \\ u_{22}^* &= \left\{r_2\left(1 - \frac{p_s^*}{\eta+(1-m)n^*}\right) - ep_i^* - d_2\right\} \\ &\quad - \frac{r_2 p_s^*}{\eta+(1-m)n^*}, \\ u_{23}^* &= -ep_s^* + \frac{\beta\gamma}{(\beta+p_i^*)^2},\ u_{31}^* = 0,\ u_{32}^* = ep_i^*, \\ u_{33}^* &= \frac{\gamma p_i^*}{(\beta+p_i^*)^2}. \end{aligned}$$

The characteristic equation is obtained as:

$$\lambda^3 + D_1\lambda^2 + D_2\lambda + D_3 = 0 \tag{7}$$

with

$$\begin{aligned} D_1 &= -\left(u_{11}^* + u_{22}^* + u_{33}^*\right), \\ D_2 &= u_{22}^*u_{33}^* - u_{23}^*u_{32}^* + u_{11}^*u_{33}^* + u_{11}^*u_{22}^* - u_{12}^*u_{21}^*, \\ D_3 &= u_{11}^*\left(u_{23}^*u_{32}^* - u_{22}^*u_{33}^*\right) + u_{12}^*\left(u_{21}^*u_{33}^*\right) - u_{13}^*\left(u_{21}^*u_{32}^*\right). \end{aligned}$$

According to the *Routh-Hurwitz* criterion, the equilibrium point $E^*$ is asymptotically stable if and only if $D_1 > 0$, $D_3 > 0$ and $D_1D_2 - D_3 > 0$. It is evident that $D_1 > 0$ when condition (*i*) holds, $D_3 > 0$ when condition (*ii*) holds and when $D_1D_2 - D_3 > 0$ condition (*iii*) holds. Therefore under the conditions specified in the theorem, equilibrium $E^*$ is locally asymptotically stable. □

## 6 Global stability analysis

In this section we analyze the global behavior of the system (1) around three vital equilibrium points $E_2$, $E_3$ and $E^*$.

### 6.1 Global behaviour around $E_2$

**Theorem 4** *The system (1) is globally asymptotically stable around the equilibrium point $E_2$ if it exists.*

***Proof*** Let us consider a set $\Psi^3_{+p_s} = \{(n, p_s, p_i) \in \mathbb{R}^3_+ : n \geq 0, ps > 0, p_i \geq 0\}$ and also consider a Lyapunov function $L_{E_2} : \Psi^3_{+p_s} \to \mathbb{R}$ around $E_2(0, \tilde{p_s}, 0)$, where $\tilde{p_s} = \frac{(r_2-d_2)\eta}{r_2}$ to prove the global stability around the equilibrium point $E_2$.

Let us assume,

$$L_{E_2} = \left(p_s - \tilde{p_s} - \tilde{p_s} \ln \frac{p_s}{\tilde{p_s}}\right)$$

$$\begin{aligned}\frac{dL_{E_2}}{dt} &= -\frac{r_2}{\eta}(p_s - \tilde{p_s})^2 \\ &< 0.\end{aligned}$$

Hence the system (1) is globally asymptotically stable around the prey and disease free equilibrium point $E_2$. □

### 6.2 Global behaviour around $E_3$

**Theorem 5** *If the equilibrium point $E_3 = (\bar{n}, \bar{p_s}, 0)$ exists then it will be globally asymptotically stable if $\frac{\alpha(1-m)^2}{(a+(1-m)n)^2} < \frac{\nu}{p_s}$.*

***Proof*** For the equilibrium point $E_3 = (\bar{n}, \bar{p_s}, 0)$, we consider $U(n, p_s) = \frac{1}{np_s}$, also consider $u_1 = \frac{r_1 n}{1+fp_s} - d_1 n - \nu n^2 - \frac{\alpha(1-m)np_s}{a+(1-m)n}$ and $u_2 = p_s\left\{r_2\left(1 - \frac{p_s}{\eta+(1-m)n}\right) - d_2\right\}$. So $U(n, p_s) > 0$ in the interior of positive quadrant of the $n - p_s$ plane. Hence,

$$\begin{aligned}\frac{\partial}{\partial n}(Uu_1) &= -\frac{\nu}{p_s} + \frac{\alpha(1-m)^2}{(a+(1-m)n)^2}, \frac{\partial}{\partial p_s}(Uu_2) \\ &= -\frac{r_2}{n(\eta+(1-m)n)}\end{aligned}$$

and

$$\begin{aligned}\Delta(n, p_s) &= \frac{\partial}{\partial n}(Uu_1) + \frac{\partial}{\partial p_s}(Uu_2) \\ &< 0.\end{aligned}$$

Due to Bendixson-Dulac criterion there exist no limit cycle in the positive quadrant of $n - p_s$ plane. Hence it will be globally asymptotically stable in positive quadrant of $n - p_s$ plane. □

### 6.3 Global behaviour around $E^*$

**Theorem 6** *The endemic equilibrium point $E^*(n^*, p_s^*, p_i^*)$ is globally asymptotically stable if the following conditions are satisfied*

$$(i)\ \nu > \frac{\alpha(1-m)^2(p_s^* + gp_i^*)}{(a+(1-m)n)(a+(1-m)n^*)},$$

$$\begin{aligned}(ii)\ &\left(\nu - \frac{\alpha(1-m)^2(p_s^* + gp_i^*)}{(a+(1-m)n)(a+(1-m)n^*)}\right) \\ &\left(d_2 + ep_i - r_2 + \frac{r_2(p_s + p_s^*)}{\eta+(1-m)n}\right) \\ &> \left(\frac{r_1 f}{2(1+fp_s)(1+fp_s^*)} + \frac{\alpha(1-m)}{2(a+(1-m)n)}\right. \\ &\left. - \frac{r_2(1-m)(p_s^*)^2}{2(\eta+(1-m)n)(\eta+(1-m)n^*)}\right)^2,\end{aligned}$$

$$\begin{aligned}(iii)\ &\left(\nu - \frac{\alpha(1-m)^2(p_s^* + gp_i^*)}{(a+(1-m)n)(a+(1-m)n^*)}\right) \\ &\left(d_2 + ep_i - r_2 + \frac{r_2(p_s + p_s^*)}{\eta+(1-m)n}\right)\frac{\gamma}{(\beta+p_i)(\beta+p_i^*)} \\ &+ \frac{1}{2}\left(ep_s^* - e - \frac{\gamma\beta}{(\beta+p_i)(\beta+p_i^*)}\right) \\ &\left(\frac{r_1 f}{2(1+fp_s)(1+fp_s^*)} + \frac{\alpha(1-m)}{2(a+(1-m)n)}\right. \\ &\left. - \frac{r_2(1-m)(p_s^*)^2}{2(\eta+(1-m)n)(\eta+(1-m)n^*)}\right)\frac{1}{2}\frac{\alpha g(1-m)}{a+(1-m)n} \\ &> \frac{1}{4}\left(ep_s^* - e - \frac{\gamma\beta}{(\beta+p_i)(\beta+p_i^*)}\right)^2 + \frac{1}{4}\left(\frac{\alpha g(1-m)}{a+(1-m)n}\right)^2 \\ &\left(\frac{r_1 f}{4(1+fp_s)(1+fp_s^*)} + \frac{\alpha(1-m)}{4(a+(1-m)n)}\right. \\ &\left. - \frac{r_2(1-m)(p_s^*)^2}{4(\eta+(1-m)n)(\eta+(1-m)n^*)}\right)^2.\end{aligned}$$

***Proof*** Let us consider the following positive definite function around $E^*$ as of the form:

$$\begin{aligned}L_{E^*} &= \left(n - n^* - n^* \ln \frac{n}{n^*}\right) \\ &+ \frac{1}{2}\left(p_s - p_s^*\right)^2 + \left(p_i - p_i^* - p_i^* \ln \frac{p_i}{p_i^*}\right).\end{aligned}$$

Differentiating $L_{E^*}$ with respect to the time variable $t$ along the solution of (1), a little algebraic calculation yields

$$\begin{aligned}\frac{dL_{E^*}}{dt} &= -[A(n-n^*)^2 + B(p_s - p_s^*)^2 + C(p_i - p_i^*)^2 \\ &+ 2H(n-n^*)(p_s - p_s^*) \\ &+ 2F(p_s - p_s^*)(p_i - p_i^*) + 2G(p_i - p_i^*)(n-n^*)] \\ &= -U^T QU,\end{aligned}$$

where $U = (n - n^*, p_s - p_s^*, p_i - p_i^*)^T$ and $Q$ is the symmetric quadratic form given by

$$Q = \begin{pmatrix} A & H & G \\ H & B & F \\ G & F & C \end{pmatrix},$$

with

$$A = \nu - \frac{\alpha(1-m)^2(p_s^* + gp_i^*)}{(a+(1-m)n)(a+(1-m)n^*)},$$
$$B = d_2 + ep_i - r_2 + \frac{r_2(p_s + p_s^*)}{\eta + (1-m)n},$$
$$C = -\frac{\gamma}{(\beta + p_i)(\beta + p_i^*)},$$
$$H = \frac{1}{2}\left\{\frac{r_1 f}{(1+fp_s)(1+fp_s^*)} + \frac{\alpha(1-m)}{a+(1-m)n} - \frac{r_2(1-m)p_s^{*2}}{(\eta+(1-m)n)(\eta+(1-m)n^*)}\right\},$$
$$F = \frac{1}{2}\left\{ep_s^* - e - \frac{\gamma\beta}{(\beta+p_i)(\beta+p_i^*)}\right\},$$
$$G = \frac{1}{2}\left\{\frac{\alpha g(1-m)}{a+(1-m)n}\right\}.$$

$Q$ is positive definite if $A > 0$, $AB - H^2 > 0$ and $det\, Q > 0$. Now $A > 0$ if condition $(i)$ holds, $AB - H^2 > 0$ if condition $(ii)$ holds and finally $det\, Q > 0$ if condition $(iii)$ holds. So, it's noted that under given conditions specified in the theorem, $Q$ is positive definite matrix, then $\frac{dL_{E^*}}{dt}$ will be negative definite. Hence $E^*$ is globally asymptotically stable according to the Lyapunov stability theorem. □

## 7 Bifurcation analysis

1. The system (1) experience a transcritical bifurcation around $E_2$.

**Theorem 7** *The system (1) goes into the transcritical bifurcation around the prey and disease free equilibrium point $E_2$ at $r_1 = r_1^{[TC_2]}$.*

***Proof*** The $|J(E_2)| = 0$ if and only if one of the eigenvalues must be zero, which leads $r_1 = r_1^{[TC_2]}$, where $r_1^{[TC_2]} = \left(\frac{d_1}{r_2} + \frac{\alpha(1-m)(r_2-d_2)\eta}{ar_2^2}\right)(r_2 + f(r_2 - d_2)\eta)$.

Let us consider the eigenvectors $\theta_3$ and $\delta_3$ corresponding to the eigenvalue 0 of the matrix $J(E_2)$ and $J(E_2)^T$.

We obtained that $\theta_3 = (\theta_1^{[3]}, \theta_2^{[3]}, 0)$, $\delta_3 = (\delta_1^{[3]}, 0, 0)$, where $\theta_1^{[3]} = \frac{r_2}{(1-m)(r_2-d_2)}\theta_2^{[3]}$, and $\theta_2^{[3]}$, $\delta_1^{[3]}$ are nonzero constants. We consider the function $F_{r_1} = \begin{pmatrix} \frac{n}{1+fp_s} \\ 0 \\ 0 \end{pmatrix}$.

Now we verify the transversality conditions using Sotomayor theorem [48].

(i) $\delta_3^T[F_{r_1}(E_2, r_1^{[TC_2]})] = 0$,

(ii) $\delta_3^T[DF_{r_1}(E_2, r_1^{[TC_2]})\theta_3] = \frac{\delta_1^{[3]}\theta_1^{[3]}r_2}{r_2 + (r_2 - d_2)f\eta} \neq 0$,

(iii) $\delta_3^T[D^2F_{r_1}(E_2, r_1^{[TC_1]})(\theta_3, \theta_3)] \neq 0$.

Therefore, all the transversality conditions for the transcritical bifurcation are verified, so the theorem holds. □

2. The system (1) shows three kinds of bifurcation around $E_3$

**Theorem 8** *(a) The system (1) attains a saddle-node bifurcation around the disease free equilibrium point $E_3$, at $r_1 = r_1^{[SN]}$, where*

$$r_1^{[SN]} = \left[\left(\frac{\alpha(1-m)^2\bar{p}_s}{(a+(1-m)\bar{n})^2} - \nu\right)\left(\frac{2r_2\bar{p}_s}{\eta+(1-m)\bar{n}} - (r_2 - d_2)\right) - \frac{r_2\alpha(1-m)^2\bar{p}_s{}^2}{(\eta+(1-m)\bar{n})^2(a+(1-m)\bar{n})}\right]\frac{1}{\chi}$$

*with* $\chi = \frac{fr_2(1-m)\bar{p}_s{}^2}{(\eta+(1-m)\bar{n})^2(1+f\bar{p}_s)^2}$.

*(b) The system (1) experiences a transcritical bifurcation around the equilibrium point $E_3$ at $e = e^{[TC_1]}$, where $e^{[TC_1]} = \frac{\beta d_3 + \gamma}{e\beta}$.*

*(c) The system (1) enters into Hopf-bifurcation around the equilibrium point $E_3$ at $\alpha = \alpha^{[HB_1]}$, when $u_{11}^2 + u_{12}u_{21} < 0$.*

***Proof*** The Jacobian matrix of the system (1) around the disease free equilibrium point $E_3$ is

$$J(E_3) = \begin{pmatrix} u_{11}^{[3]} & u_{12}^{[3]} & u_{13}^{[3]} \\ u_{21}^{[3]} & u_{22}^{[3]} & u_{23}^{[3]} \\ 0 & 0 & u_{33}^{[3]} \end{pmatrix}.$$

(a) $J(E_3)$ has a zero eigenvalue if and only if $|J(E_3)| = 0$ that gives us $r_1 = r_1^{[SN]}$. The other two eigenvalues evaluated from the characteristic of the Jacobian for $r_1 = r_1^{[SN]}$ and one of them should be negative from

the two non zero eigenvalues in order to get a saddle-node bifurcation.

Let us consider two eigen vectors $\theta_1$ and $\delta_1$ corresponding to the eigenvalue 0 for the matrix $J(E_3)$ and its transpose, respectively.

We find that $\theta_1 = (\theta_1^{[1]}, \theta_2^{[1]}, 0)^T, \delta_1 = (\delta_1^{[1]}, \delta_2^{[1]}, \delta_3^{[1]})^T$, where $\theta_1^{[1]} = -\frac{u_{12}^{[3]}}{u_{11}^{[3]}}\theta_2^{[1]}$, $\delta_1^{[1]} = -\frac{u_{21}^{[3]}}{u_{11}^{[3]}}\delta_2^{[1]}$, $\delta_3^{[1]} = \left(\frac{u_{21}^{[3]}u_{13}^{[3]}}{u_{11}^{[3]}u_{33}^{[3]}} - \frac{u_{23}^{[3]}}{u_{33}^{[3]}}\right)\delta_2^{[1]}$ and here $\theta_2^{[1]}, \delta_2^{[1]}$ are nonzero constants. Taking the function $F_{r_1} = \begin{pmatrix} \frac{n}{1+fp_s} \\ 0 \\ 0 \end{pmatrix}$, and hence

(i) $\delta_1^T[F_{r_1}(E_3, r_1^{[SN]})] = \dfrac{\bar{n}\delta_1^{[1]}}{1+f\bar{p}_s} \neq 0,$

(ii) $\delta_1^T[D^2F_{r_1}(E_3, r_1^{[SN]})(\theta_1, \theta_1)] \neq 0.$

Therefore, according to [48] the system (1) experiences a saddle node bifurcation around the disease free equilibrium point $E_3$ at $r_1 = r_1^{[SN]}$.

(b) To established the transcritical bifurcation of the system (1) around the disease free equilibrium point $E_3$, consider two eigen vectors $\theta_2$ and $\delta_2$ corresponding to the eigen value 0 of the matrix $J(E_3)$ and transpose of $J(E_3)$.

We obtained that the representation of the eigen vector are $\theta_2 = (\theta_1^{[2]}, \theta_2^{[2]}, \theta_3^{[2]})^T$, $\delta_2 = (0, 0, \delta_3^{[2]})^T$, where $\theta_1^{[2]}$, $\theta_2^{[2]}$, $\theta_3^{[2]}$ and $\delta_3^{[2]}$ are nonzero constants. At the equilibrium point $E_3$ for the parameter $e = e^{[TC_1]}$, and the function represented as $F_e = \begin{pmatrix} 0 \\ -p_s p_i \\ p_s p_i \end{pmatrix}$, we have

(i) $\delta_2^T[F_e(E_3, e^{[TC_1]})] = 0,$

(ii) $\delta_2^T[DF_e(E_3, e^{[TC_1]})\theta_2] = \delta_3^{[2]}\theta_3^{[2]}\bar{p}_s \neq 0,$

(ii) $\delta_2^T[D^2F_e(E_3, e^{[TC_1]})(\theta_2, \theta_2)] \neq 0.$

According to [48] system (1) attains a transcritical bifurcation around the disease free equilibrium point $E_3$ at $e = e^{[TC_1]} = \frac{\beta d_3 + \gamma}{e\beta}$.

(c) From the characteristic equation (6), the eigenvalues are given by

$$\lambda_{1,2} = \frac{1}{2}\left[(u_{11}^{[3]} + u_{22}^{[3]}) \pm \sqrt{(u_{11}^{[3]} + u_{22}^{[3]})^2 - 4(u_{11}^{[3]}u_{22}^{[3]} - u_{12}^{[3]}u_{21}^{[3]})}\right],$$

$$\lambda_3 = e\bar{p}_s - \frac{\gamma}{\beta} - d_3.$$

It is clear that $\lambda_3$ is a real root, so $\lambda_1$ and $\lambda_2$ are purely imaginary if there exist an

$$\alpha = \left(\frac{2r_2\bar{p}_s}{\eta + (1-m)\bar{n}} + \nu\bar{n} - (r_2 - d_2)\right)$$
$$\frac{(a+(1-m)\bar{n})^2}{(1-m)^2\bar{n}\bar{p}_s} = \alpha^{[HB_1]}.$$

Furthermore,

$$\left[\frac{d(Re\lambda_i)}{d\alpha}\right]_{\alpha=\alpha^{[HB_1]}} = \frac{(1-m)^2\bar{n}\bar{p}_s}{(a+(1-m)\bar{n})^2} \neq 0, \quad i = 1, 2.$$

Therefore the system (1) attains a Hopf-bifurcation around the disease free equilibrium point $E_3$ for $\alpha = \alpha^{[HB_1]}$, where $\alpha^{[HB_1]} = \left(\frac{2r_2\bar{p}_s}{\eta+(1-m)\bar{n}} + \nu\bar{n} - (r_2 - d_2)\right)$ $\frac{(a+(1-m)\bar{n})^2}{(1-m)^2\bar{n}\bar{p}_s}$. □

3. In our study, the growth rate of susceptible predator is one of the most vital parameter. So we choose $r_2$ as a bifurcation parameter. Now we established the conditions for the occurrence of Hopf bifurcations at positive interior equilibrium point $E^*$ with respect to the growth rate of susceptible predator parameter $r_2$.

**Theorem 9** *When the growth rate of susceptible predator coefficient $r_2$ crosses a critical value $r_2^*$, the system (1) undergoes a Hopf bifurcation around the positive interior equilibrium $E^*$ if the following conditions are satisfied:*

*(i)* $D_1(r_2^*) > 0,\ D_3(r_2^*) > 0,$

*(ii)* $\triangle(r_2^*) = D_1(r_2^*)D_2(r_2^*) - D_3(r_2^*) = 0,$

*(iii)* $\left.\frac{d\triangle(r_2^*)}{dr_2}\right|_{r_2=r_2^*} \neq 0.$

***Proof*** The characteristic equation (7) can also be written as,

$$\lambda^3 + D_1(r_2)\lambda^2 + D_2(r_2)\lambda + D_3(r_2) = 0.$$

If $\triangle(r_2^*) = D_1(r_2^*)D_2(r_2^*) - D_3(r_2^*) = 0$ for $r_2 = r_2^*$, then the characteristic equation (7) must be of the form

$$\left[\lambda^2(r_2^*) + D_2(r_2^*)\right]\left[\lambda(r_2^*) + D_1(r_2^*)\right] = 0. \tag{8}$$

Equation (8) has roots $\lambda_1(r_2^*) = i\sqrt{D_2(r_2^*)}$, $\lambda_2(r_2^*) = -i\sqrt{D_2(r_2^*)}$, $\lambda_3(r_2^*) = -D_1(r_2^*) < 0$, since $D_1(r_2^*) > 0$, $D_3(r_2^*) > 0$. Now, we need to validate the transversality condition:

$$\left[\frac{d(Re\lambda_j(r_2))}{dr_2}\right]_{r_2=r_2^*} \neq 0, \ j = 1, 2.$$

Substituting $\lambda_j(r_2) = p_1(r_2) \pm p_2(r_2)$ into equation (8) and calculating derivative, we have

$$G(r_2)p_1'(r_2) - H(r_2)p_2'(r_2) + I(r_2) = 0, \tag{9}$$
$$G(r_2)p_2'(r_2) + H(r_2)p_1'(r_2) + J(r_2) = 0, \tag{10}$$

where

$$\begin{aligned}
G(r_2) &= 3p_1^2(r_2) - 3p_2^2(r_2) + 2p_1(r_2)D_1(r_2) + D_2(r_2),\\
H(r_2) &= 6p_1(r_2)p_2(r_2) + 2D_1(r_2)p_2(r_2),\\
I(r_2) &= D_2'(r_2)p_1(r_2) - D_1'(r_2)p_2^2(r_2) + p_1^2(r_2)D_1'(r_2) + D_3'(r_2),\\
J(r_2) &= 2p_1(r_2)p_2(r_2)D_1'(r_2) + D_2'(r_2)p_2(r_2).
\end{aligned}$$

Here, $p_1(r_2^*) = 0,\ p_2(r_2^*) = \sqrt{D_2(r_2^*)}$. Hence, we have

$$\begin{aligned}
&G(r_2^*) = -2D_2(r_2^*),\ H(r_2^*) = 2D_1(r_2^*)\sqrt{D_2(r_2^*)},\\
&I(r_2^*) = D_3'(r_2^*) - D_1'(r_2^*)D_2(r_2^*),\ J(r_2^*) = D_2'(r_2^*)\sqrt{D_2(r_2^*)}.
\end{aligned}$$

Solving for $p_1'(r_2)$, from equations (9) and (10), we have

$$\begin{aligned}
\left[\frac{dRe(\lambda_j(r_2))}{dr_2}\right]_{r_2=r_2^*} &= p_1'(r_2^*) = -\frac{H(r_2^*)J(r_2^*)+G(r_2^*)I(r_2^*)}{G^2(r_2^*)+H^2(r_2^*)}\\
&= \frac{D_3'(r_2^*) - D_1(r_2^*)D_2'(r_2^*) - D_1'(r_2^*)D_2(r_2^*)}{2(D_1^2(r_2^*) + D_2^2(r_2^*))}.
\end{aligned}$$

If $\frac{d}{dr_2}[D_1(r_2)D_2(r_2) - D_3(r_2)]_{r_2=r_2^*} \neq 0$ then the transversality condition $\frac{d\triangle(r_2)}{dr_2}\Big|_{r_2=r_2^*} \neq 0$ holds. This implies that a Hopf bifurcation occurs at $r_2 = r_2^*$ provided the conditions stated in the theorem are satisfied. □

## 8 Sensitivity analysis (PRCC)

To understand species interactions, we develop and analyze mathematical models characterized by several variables, parameters, and constraints, many of which are uncertain due to challenges in experimental measurement or even completely unknow in some cases. Consequently, addressing these uncertainties naturally becomes an integral aspect of the process. Uncertainty and sensitivity analyses aid in assessing and managing these uncertainties. Among the non-stratified sampling methodologies, we utilize the Latin Hypercube Sampling (LHS). The LHS technique ensures a comprehensive and efficient sampling strategy by dividing the parameter space into non overlapping intervals, which prevents redundant sampling and enhances the exploration of uncertainty ranges. Additionally, by combining LHS with Partial Rank Correlation Coefficient (PRCC), we gain deeper insights into the interplay between parameter variations and model outputs, enabling us to pinpoint critical factors driving system dynamics. This integration not only highlights the individual influence of parameters but also we assume uniform distributions for all parameters when generating the Latin Hypercube Sampling (LHS) matrices. Subsequently, 500 simulations of the system are conducted utilizing the same base- line values. Parameters are permitted to vary within ±25% of these levels. The statistical method of PRCC evaluates the degree of correlation between input parameters and model output, yielding a value within the range of [−0.3, 0.3], with the sign indicating the correlation type and the value representing its strength. Figure 1 presents a visual representation of the PRCC values associated with each model parameter, with infected predator biomass acting as the response function. Within this framework, we classify the key parameters influencing the augmentation of infected predator biomass into two distinct categories: those that positively contribute to biomass enhancement (positive PRCC values) and those that result in a reduction of infected predator biomass (negative PRCC values).

The figure separately illustrates the impact of the parameters positively and negatively, that the parameters positively impacted the infected predator biomass, namely $r_1, d_1, m, g, a, r_2, \eta$ and $e$ featuring their significant contributions to the enhancement of infected predator biomass, while the model parameters with negatively impacted on the infected predator biomass include $f, \nu, \alpha, d_2, \gamma$ and $d_3$. Therefore, the central focus lies in understanding how the disease transmission rate ($e$), consumption rate ($\alpha$), growth rate of predator species ($r_2$), intra-species competition ($\nu$), the treatment effect ($\gamma$) and the natural death rate of susceptible predator ($d_2$) leverage the overall dynamical configuration and the biomass of interacting species.

The violin Fig. 2 provides a comprehensive visualization of the distribution and reliability of PRCC values through bootstrapped simulation. Vertical length of each violin indicate the central tendency i.e., the direction as well as strength of the parameter influence and the horizontal spread of the violin indicates the stability and variability of that influence.

It is clear from the Fig. 2, negatively centered violins formed corresponding to the parameters $f, \nu, \alpha, g, r_2, \beta$ and $d_3$ reflect a strong consistent suppressive effect on infected predator biomass. In a similar way we identify the parameters $r_1$, $m$, $a$, $\eta$ and $e$ exhibit positively centered violins, indicating stable positive contribution to the level of infection. Along with that some of the parameter centered near zero like $d_1$, $d_2$ and $\gamma$ indicating comparatively weak and uncertain influence with higher variability across samples. The parameters $\alpha$, $e$, $\beta$ and $d_3$ greater width indicates the stability around the centered of violin. By examining height (strength and direction of influence), width (variability across sample) of every violin not only the ranks of the parameters by their importance but also reveals the consistency of each parameter effect in the system (1) dynamics.

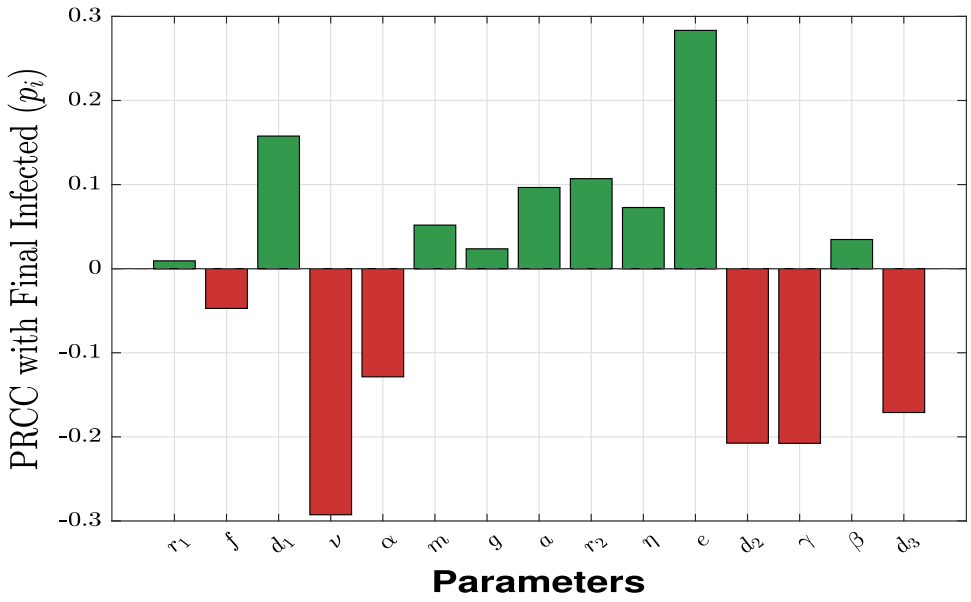


**Fig. 1** PRCC results capturing the sensitivity indices of parameters with infected predator biomass. The infected predator biomass exhibits significant variability with changes in the parameters $e, \nu, \gamma, d_2, \alpha$ and $r_2$. This identifies key model parameters essential for the qualitative analysis of the system (1)

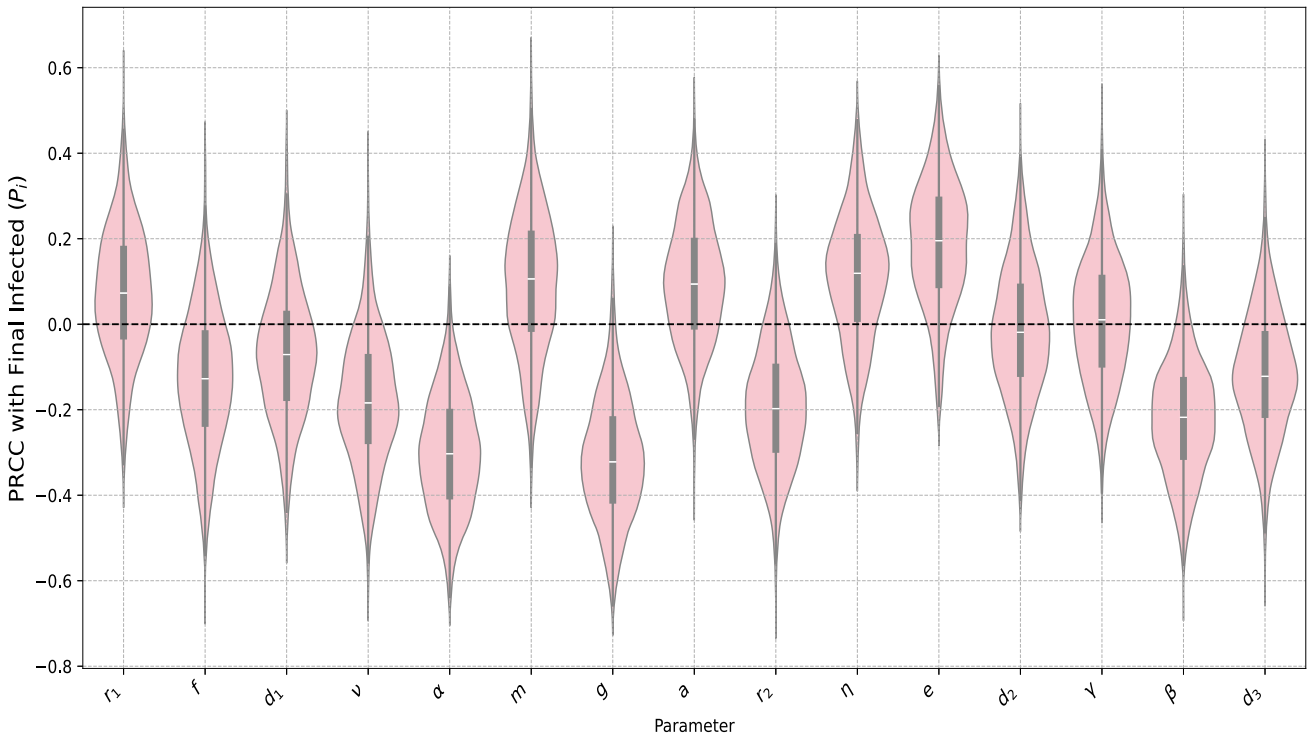


**Fig. 2** Violin plot of PRCC values for system (1) w.r.t parameter (Generated distribution around PRCC valued)

## 9 Normalized Sensitivity analysis of $\mathcal{R}_0$

To analyze the influence of various parameters on the basic reproduction number ($\mathcal{R}_0$) in the system (1), we used normalized sensitivity index to know the influence of parameters on the reproduction number, it's a very significant way to identify the parameters which is more affect the system (1) for spreading the infection. In our model $\mathcal{R}_0$ defined as,

$$\mathcal{R}_0 = \frac{e\beta\bar{p}_s}{\beta d_3 + \gamma}.$$

The normalized sensitivity index for any parameter $\Gamma$ provides a measure of how sensitive $\mathcal{R}_0$ is to change in $\Gamma$. This sensitivity index is computed as:

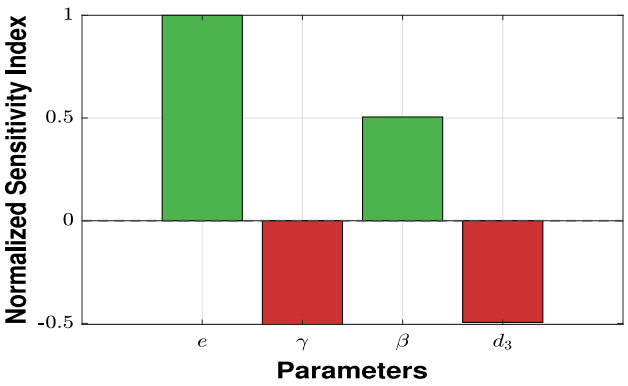


**Fig. 3** Normalized sensitivity

$$S^{\Gamma}_{\mathcal{R}_0} = \frac{\partial \mathcal{R}_0}{\partial \Gamma}\frac{\Gamma}{\mathcal{R}_0}.$$

This approach is valuable as it quantifies the relative effect of each parameter on the basic reproduction number $\mathcal{R}_0$, provide insight into which factors most significantly influence the system's dynamics. Sensitivity analysis thus influence us to focus on parameters that have the strongest impact on the system's nature, which is crucial for understanding disease transmission. The normalized sensitivity indices for the parameters, which have a impact on $\mathcal{R}_0$ from the system (1), are calculating using the above mathematical expression and also generated the graph using the parametric value mentioned in the Table 1

$$S^{e}_{\mathcal{R}_0} = 1, \quad S^{\beta}_{\mathcal{R}_0} = 0.5, \quad S^{d_2}_{\mathcal{R}_0} = -0.5, \quad S^{d_3}_{\mathcal{R}_0} = -0.5.$$

Nevertheless the sensitivity calculation of other parameters like $r_1$, $f$, $d_1$, $\nu$, $\alpha$, $m$, $a$, $g$, $r_2$, and $d_2$ is extremely cumbersome and tedious to be determined, due to the density of susceptible predator species at the infection free equilibrium point. So we have calculate the sensitivity indices of $\mathcal{R}_0$ with respect to the some specific parameters of the system (1) also represent the graphical structure in Fig. 3. It's very natural also biologically evident that $\mathcal{R}_0$ is most positively sensitive for the disease transmission rate ($e$), i.e., which indicates that the increment of the value of $e$ grow the value of $\mathcal{R}_0$ then the result of that particular scenario raise the infections. On the other hand the basic reproduction number negatively sensitive for the parameter $\gamma$ which indicates that the increment of $\gamma$ decrease the value of $\mathcal{R}_0$, so if we increase the value of $\gamma$ that can be prevent the spreads of disease.

We also study and plot 3D diagram in the presence of predator species along with the two other parameters effect on the reproduction number of the system (1). Our numerical study suggests that in the presence of alternating food resources the susceptible predator can't goes to the extinction, to keep in mind all the circumstances we consider the range of $p_s \in [0.6, 6]$. Here we measure the reproduction using the color and a specific color is represent the specific number.

In Fig. 4a it is noticed that the disease transmission rate $e$ and susceptible predator ($p_s$) presence in a high density helps to increase the reproduction number. It is also visible that the increased of death rate of infected predator species ($d_3$) helps to reduce the reproduction number and small value of $e$ along with controllable presence of $p_s$ reduce the reproduction number. Figure 4b represents the reproduction number ($\mathcal{R}_0$) is very high only when the disease transmission rate ($e$) is very high and highly presence of susceptible predator species ($p_s$). The treatment effect ($\gamma$) is effective enough to control the reproduction number ($\mathcal{R}_0$) in highly spreading situation. Figure 4c shows that delay of treatment makes help to sustain reproduction number ($\mathcal{R}_0$) in a high density. It gradually decreased due to the treatment pressure. Figure 4d shows that high level of reproduction possible only when the death rate of predator species ($d_3$) and the treatment effect ($\gamma$) operate in a low level.

## 10 Optimal control

In natural ecosystems, it is generally not possible to directly treat all affected predators. In our framework, the control variable $\gamma(t)$ represents a generalized intervention effort such as disease management through vaccination, supplementary feeding or habitat based control measures rather than literal treatment of individual animals. The purpose of this optimal control analysis is to explore how management intensity could be adjusted over time to minimize infection and control related costs, thereby providing theoretical guidance for sustainable ecosystem management. A problem of optimal control is considered in which the objective function constructed as follows:

$$Z(\gamma) = \int_0^T (\xi p_i(t) + \phi\gamma^2(t))dt.$$

Here, $\xi$, $\phi$ are represented as weighted per capita constants that quantify the reduction the presence of infected population as well as the treatment of infected individuals and T is the treatment duration.

Hence, the optimal control issue being studied is to determine the optimal $\gamma^*(t)$ in such a way that

$$\begin{aligned} Z(\gamma^*(t)) &= min\{Z(\gamma) : \gamma \in W\}, \quad \text{where} \\ W &= \{\gamma(t) : 0 \le \gamma(t) \le 2, t \in [0, T]\}, \end{aligned}$$

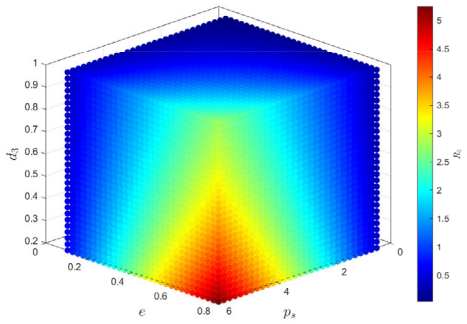

(a) Measure the reproduction number for changes of disease transmission rate $e$ and death rate of infected predator $d_3$

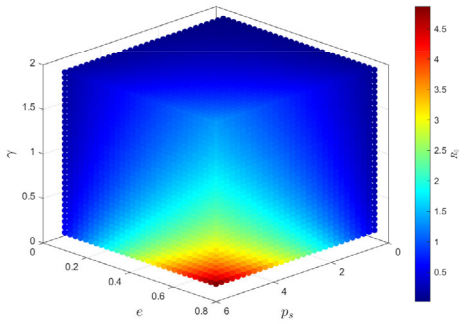

(b) Measure the reproduction number for changes of disease transmission rate $e$ and medical resources for treatment $\gamma$

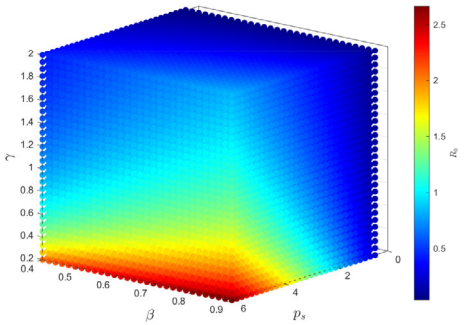

(c) Measure the reproduction number for changes of delayed treatment parameter $\beta$ and medical resources for treatment $\gamma$

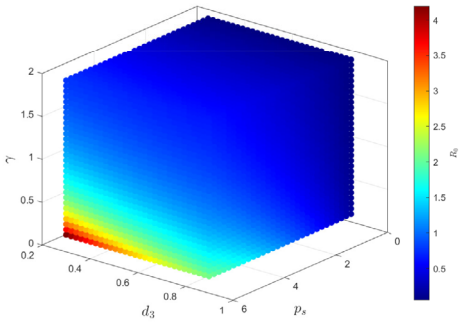

(d) Measure the reproduction number for changes of death rate of infected predator $d_3$ and medical resources for treatment $\gamma$

**Fig. 4** 3D diagram to measure the reproduction number $\mathcal{R}_0$

In our optimization problem, we construct the Hamiltonian function as

$$H(n, p_s, p_i, \gamma, \psi_1, \psi_2, \psi_3) = \xi p_i(t) + \phi\gamma^2(t) + \sum_{i=0}^{3} \psi_i f_i.$$

Using the Pontryagin's maximum principle, the adjoint equations are given by

$$\frac{d\psi_1}{dt} = -\frac{\partial H}{\partial n}, \quad \frac{d\psi_2}{dt} = -\frac{\partial H}{\partial p_s} \quad \text{and} \quad \frac{d\psi_3}{dt} = -\frac{\partial H}{\partial p_i}$$

with the transversality conditions $\psi_i(T) = 0, i = 1(1)3$.

Therefore,

$$\begin{aligned}
\frac{d\psi_1}{dt} &= -\psi_1\left[\frac{r_1}{1+fp_s} - d_1 - 2\nu n - \frac{\alpha(1-m)}{(a+(1-m)n)^2}(p_s + gp_i)\right] \\
&\quad -\psi_2\left(\frac{p_s^2(1-m)r_2}{(\eta+(1-m)n)^2}\right), \\
\frac{d\psi_2}{dt} &= \psi_1\left[\frac{r_1 fn}{(1+fp_s)^2} + \frac{\alpha(1-m)n}{a+n(1-m)}\right] \\
&\quad -\psi_2\left[r_2\left(1 - \frac{2p_s}{\eta+(1-m)n}\right) - ep_i - d_2\right] - \psi_3\left[ep_i\right], \\
\frac{d\psi_3}{dt} &= -\xi + \psi_1\left(\frac{\alpha(1-m)gn}{a+(1-m)n}\right) + (\psi_2 - \psi_3)ep_s \\
&\quad +(\psi_3 - \psi_2)\frac{\gamma\beta}{(\beta+p_i)^2} + \psi_3 d_3.
\end{aligned} \tag{11}$$

Now using the optimality condition $\frac{\partial H}{\partial \gamma} = 0$, we find $\gamma = \frac{p_i(\psi_3-\psi_2)}{2\phi(\beta+p_i)}$.

Thus the following optimum control variable is obtained

$$\gamma^* = min\left(2, max\left(0, \frac{p_i(\psi_3 - \psi_2)}{2\phi(\beta + p_i)}\right)\right).$$

## 11 Numerical simulation

In this context, we demonstrate comprehensive numerical simulations aimed at unveiling the intricate dynamical behaviors of the system (1). We utilize MATLAB's ode45 solver to generate time series representation of the system (1) to

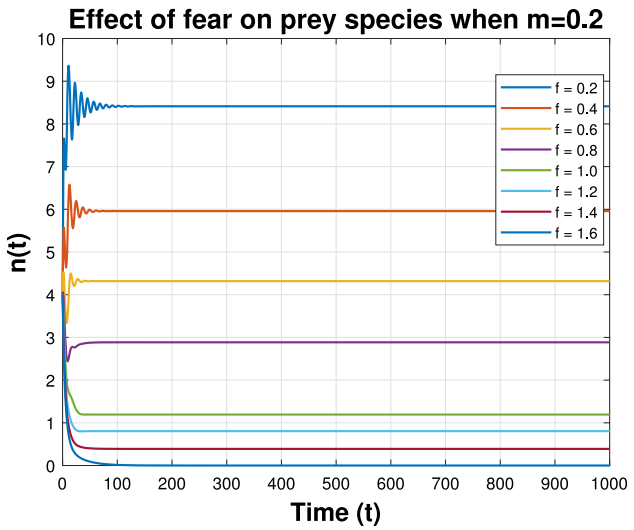


**Fig. 5** Influence of fear effect $f$ on prey population of the system (1) when refuge $m = 0.2$

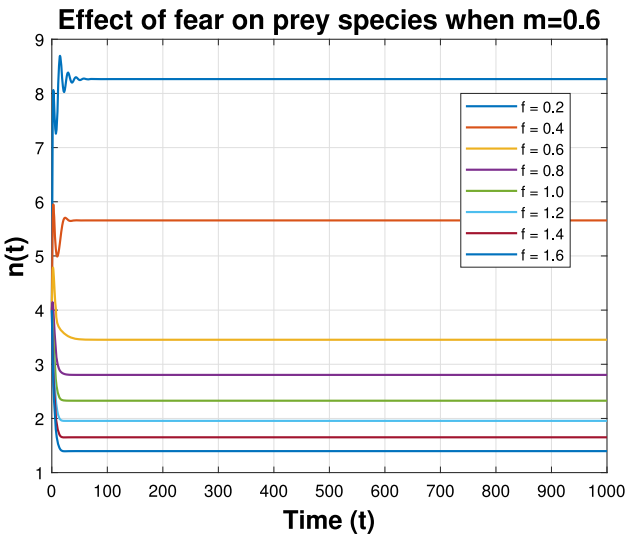


**Fig. 6** Influence of fear effect $f$ on prey population of the system (1) when refuge $m = 0.6$

track changes in the steady-state behaviors of interacting populations and also the global stability. Along with that generate contour diagrams, which triggered the numerical study to interpret the biomass of any species for simultaneously changes of two parameter values. Further we perform single and multiple parameter bifurcation diagrams using MatCont within MATLAB software.

### 11.1 Impact of prey biomass on predator induced fear ($f$) and prey refuge ($m$)

In this section, we investigate the effect of fear ($f$) on prey species of the system (1) for different values of prey refuge ($m$). The increment of fear in prey ($n$) population with the low refuge rate $m = 0.2$ leads to extinction the prey population ($n$) for $f = 1.6$ (see Fig. 5). It is also clear from Fig. 5 that proliferation of fear in prey species gradually decrease the biomass of prey and a certain threshold value, the system becomes prey free.

Now we increase the refuge amount from $m = 0.2$ to $m = 0.6$ and other parameters value taken from Table 1 except $f$. For that change make an insightful impact on prey species, leads to protect from the extinction of prey for $f = 1.6$ (see Fig. 6). Further increase of refuge amount $m = 0.8$ helps to sustain the prey species for higher value of fear $f = 1.6$ with sufficient amount of biomass (see Fig. 7).

Figure 8 ensure that the presence of prey refuge ($m$), helps to protect prey species from extinction. As well as for sensible amount of intra-species competition ($\nu$) reduce the biomass of prey species but not goes to the extinction. Increase the value of ($m$) system (1) shows a very fascinating dynamical phenomenon for two different values intra-species competition. If the competition rate is low $\nu = 0.0001$ and parameter

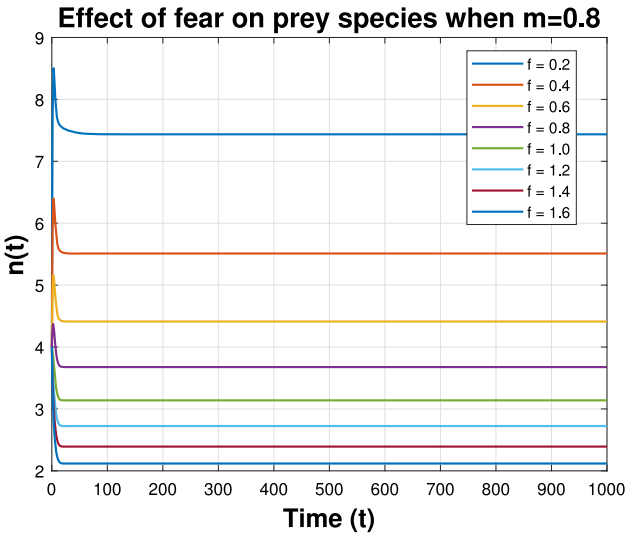


**Fig. 7** Influence of fear effect $f$ on prey population of the system (1) when refuge $m = 0.8$

values taken from Table 1, prey species sustain in a same biomass up to the value of $m = 0.8$ after crossing the threshold value $m = 0.8$ species growing very highly. For $\nu = 0.005$, the prey population remains healthy and shows a slight decrease when the refuge rate is high. Along with that for high competition rate ($\nu = 0.12$ and $\nu = 0.15$) slightly decrease the biomass of prey species for growing the refuge rate but after crossing the threshold value $m = 0.8$ increase the biomass of prey species. Finally, to know the combine effect of predation fear ($f$) and the prey refuge ($m$) on the density of prey ($n$) biomass we draw a contour diagram (see Fig. 9). The horizontal axis represents the prey refuge ($m$), vertical axis represents the fear ($f$) and the vertical color line represents the prey biomass ($n$).

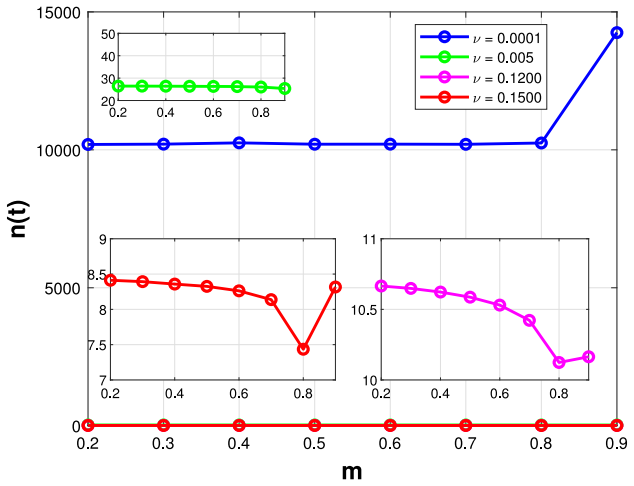


**Fig. 8** Effect of the refuge $m$ in the presence of fear $f$ for different values of intra-species competition $\nu$

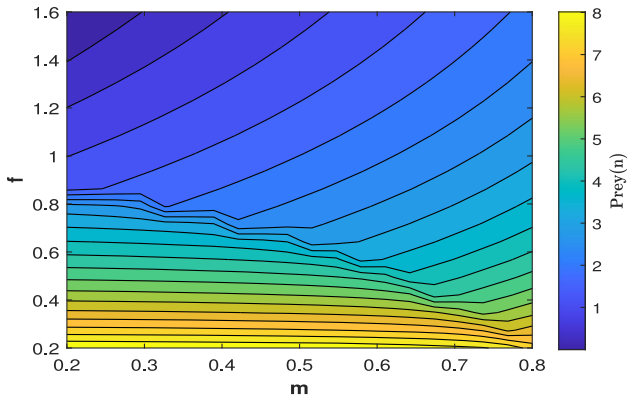


**Fig. 9** Contour diagram with respect to the parameter $m$ and $f$ to measure the biomass of prey population ($n$)

The high value of fear and low value of refuge leads to reduce the prey biomass. Although the low fear amount helps to maintain the sufficiently high amount prey species and the moderate amount of fear leads to maintain the sensible amount prey in the system (1) (see Fig. 9).

## 11.2 Bifurcation analysis

In this section we have investigated the effect of vital parameters $r_1$, $f$, $\alpha$, $m$, $r_2$, $e$ and $\gamma$ numerically on the population dynamics. The primary aim of this section is to study the dynamical nature of the model for a wide range of above parameter values. Initially we consider the parametric value mention in the Table 1 throughout, unless otherwise stated.

### 11.2.1 Role of growth rate ($r_1$) of prey species in system dynamics

To begin, we investigate the nature of the dynamics of our system (1) by drawing one parameter bifurcation with respect to the growth rate of prey species. For lower value of growth rate $r_1$ specifically $r_1 \in (0, 0.7120009)$, only the prey and disease free state $E_2$ exist, where only the susceptible predator able to sustain due to the presence of alternating food resources, despite the low growth rate of prey species. At $r_1 = 0.7120009$ the system (1) undergoes a saddle-node bifurcation where two coexisting equilibrium collide and vanish. Further increase the value of $r_1$ the system exhibits bi-stability in between $E_2$ and $E_3$ with in the range $r_1 \in (0.7120009, 0.743567824)$ depending on the initial condition. The system (1) experiences transcritical bifurcation at $r_1 = 0.743567824$. Further increase the value of $r_1$ system (1) admits a stable infection free state $E_3$ for $r_1 \in (0.743567824, 0.9297507)$ (see Fig. 10). At $r_1 = 0.9297507$ a second saddle-node bifurcation occurs, where two equilibrium points of opposite nature collide and vanish. Beyond this point for $r_1 \in (0.9297507, 1.0439525)$ the system (1) again shows bi-stability nature in between infection free ($E_3$) and endemic ($E^*$) equilibrium state contingent on initial condition and the system (1) finally at $r_1 = 1.0439525$ leads to a transcritical bifurcation, beyond which ($r_1 > 1.0439525$), the system stabilizes at an endemic equilibrium state $E^*$.

In the above discussion, we observe that the system (1) exhibits a stable endemic state for higher value of $r_1$, primarily due to available food source of the predators. Additionally, the presence of prey refuge allow the prey species to persist by offering protection from predation at higher population, comparatively low growth rate shows bi-stability in between endemic and disease free state due to weaker impact of infected predator. The system shows disease free nature when slightly decrease the growth rate. Along with that the system (1) may occur another bi-stability to slightly reduce of growth rate which depends on initial condition. In addition for lower growth rate system only persist the susceptible predator depends on the additional food resources (see Fig. 10). Mondal et al. demonstrates in their work for low value of prey growth rate exhibits the disease free stable state up to a certain value after that system undergoes oscillatory nature where infected predator remain absent. For higher value of prey growth rate stabilize the system at endemic state [10]. This result partially align with our observation.

### 11.2.2 Role of fear ($f$) on prey species in system dynamics

To investigate the role of the fear effect on prey species, we draw the one parameter bifurcation diagram of the system (1) with respect to the fear parameter $f$. For low

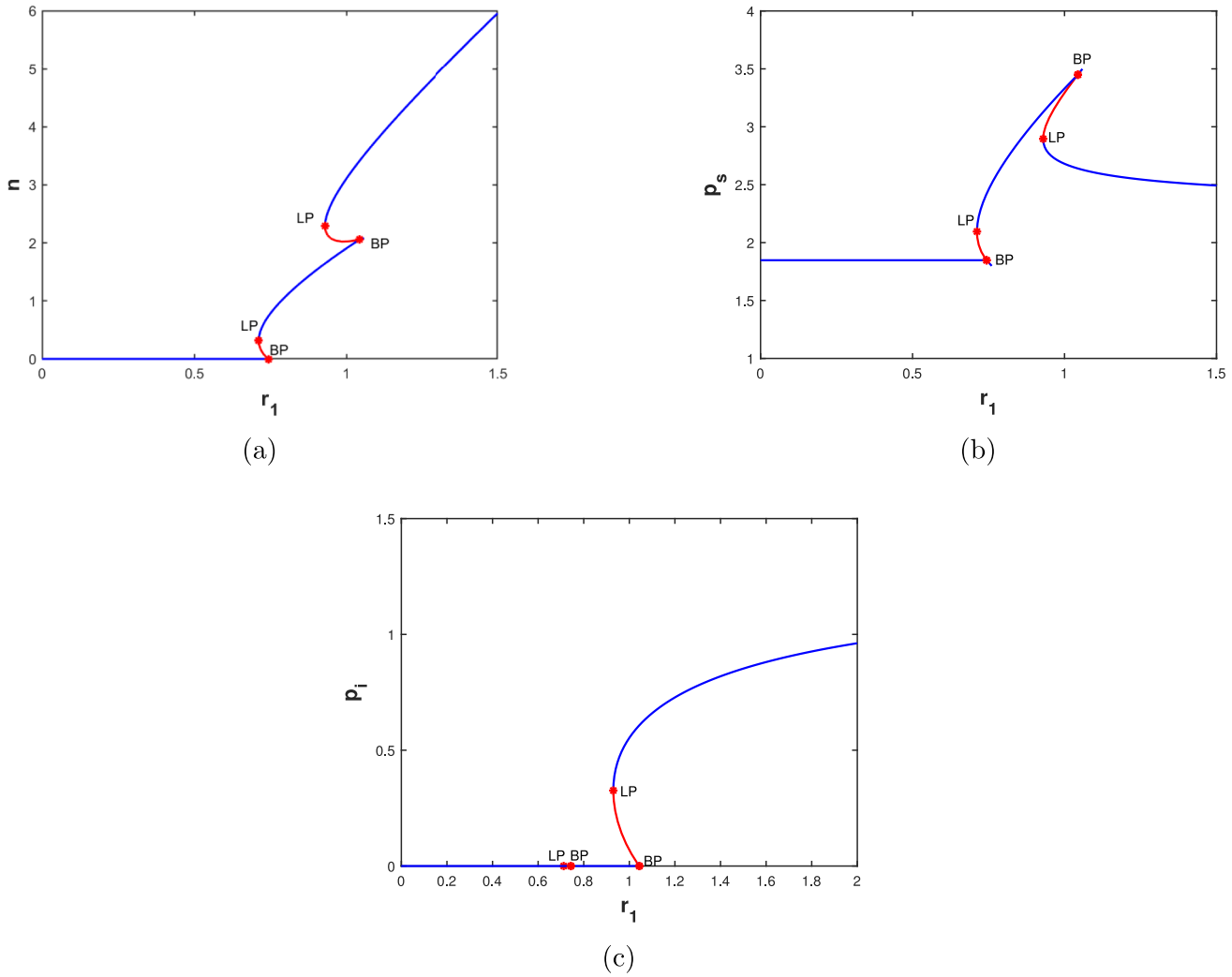


**Fig. 10** Bifurcation diagram with respect to the growth rate of prey species $r_1$

fear effect ($f < 0.6486475$) the system (1) shows stable endemic state where all the species are coexist despite the low fear effect, the system (1) undergoes a transcritical bifurcation at $f = 0.6486475$. Further increase the value of $f \in (0.6486475, 0.8317018)$ system (1) shows a bi-stability, where two types of stable nature ($E^*$ and $E_3$) exists depends on the initial condition. Also the system (1) exhibits a saddle-node bifurcation at $f = 0.8317018$ where two equilibrium points of opposite nature collide and vanish. Further increase of $f$ system (1) shows disease free state in the range $f \in (0.8317018, 1.4524291)$. At $f = 1.4524291$ system (1) undergoes a transcritical bifurcation and when the value of $f \in (1.4524291, 1.4638723)$ system (1) posses through a bi-stability nature in between ($E_3$ and $E_2$) depends on the initial condition. For $f = 1.4638723$ system (1) shows second saddle-node bifurcation where two opposite nature equilibrium point collide and vanish and finally for high value of fear ($f > 1.4638723$) system (1) goes to the prey and disease free stable state $E_2$ (see Fig. 11).

From the above illustration, we observe that for very high values of the fear ($f$) system (1) persist only the susceptible predator population, depending on the availability of alternative food sources. At slightly lower fear levels, the system may exhibit bi-stability, where both a disease free state and prey and disease free state are possible, depending on the initial conditions. For moderate fear levels the system (1) tends toward a disease free state, as the fear effect in the prey population causes a decline in prey density, leading to extinction of the weaker (infected) predator due to food scarcity. Conversely, at very low levels of fear helps to sustain the prey species in the system (1) maintains a stable endemic state, while a slight increase in fear may lead the system (1) another equilibrium state disease free stable along with stable endemic state depending on the initial conditions. Mondal et al. observed that changing the value of fear from lower to

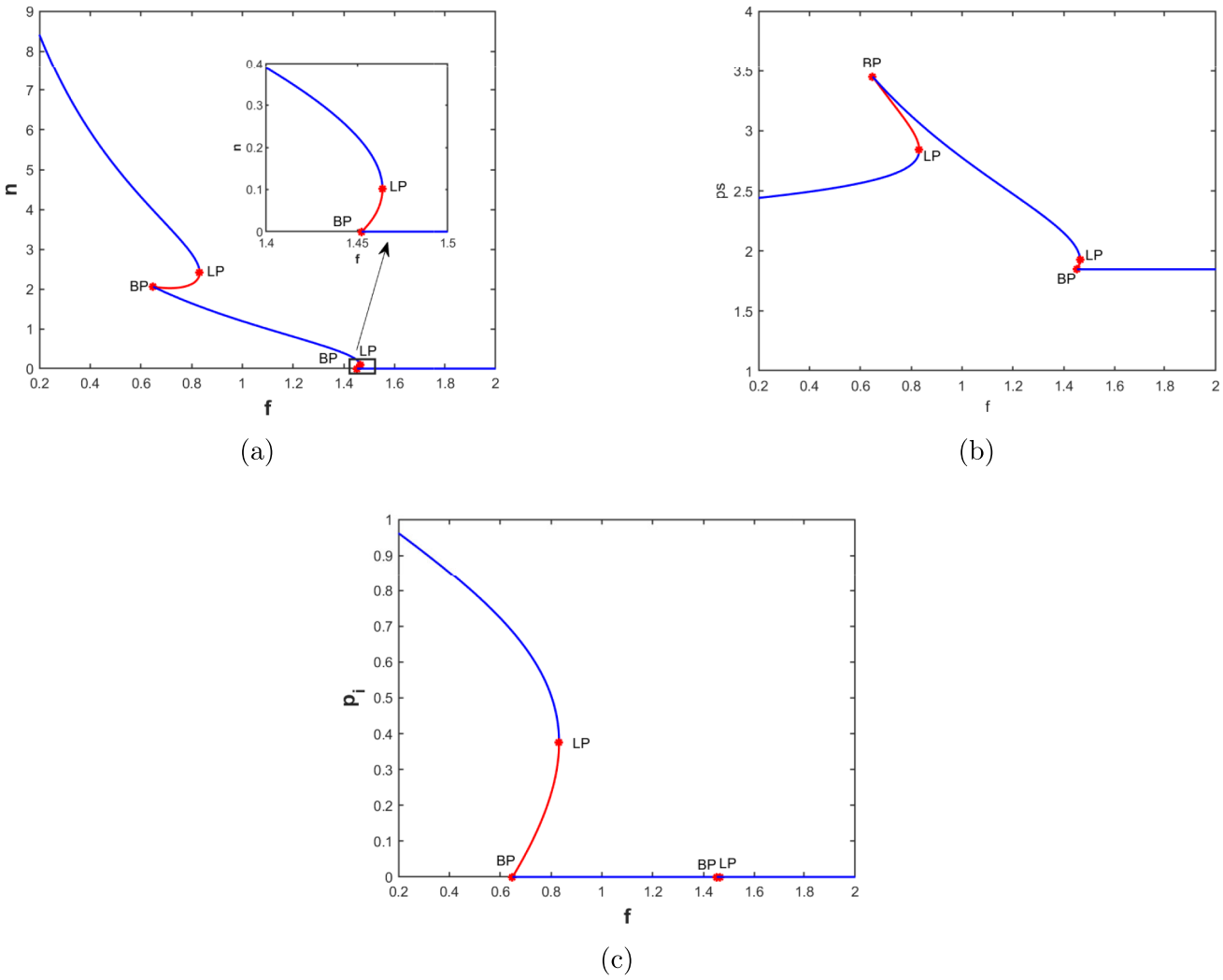


**Fig. 11** Bifurcation diagram with respect to the fear parameter $f$

higher system exhibits a stable endemic nature to an oscillatory disease free state to disease free stable state [10]. Sarkar et al. demonstrated that in their work an increase in fear does not effect significantly in the growth of prey species [32]. However, Pal observed the system exhibits chaotic nature at lower levels of fear, while higher value system showed the stable endemic nature [20]. In contrast, our study we find that extensive fear can derive the system to a disease free then disease and prey free state, while moderate level of fear result in bi-stability, and endemic for lower level of fear.

### 11.2.3 Role of consumption rate of predator species ($\alpha$) on prey species in system dynamics

To study the role of consumption rate of prey species, we draw a bifurcation diagram of the system (1) for prey species with respect to the consumption rate $\alpha$.

For lower value of $\alpha$ helps to maintain sufficient amount of prey species in the system (1), resulting in stable endemic state for $\alpha \in (0, 0.682543)$. At $\alpha = 0.682543$ system (1) undergoes a transcritical bifurcation. As $\alpha$ increase further, the system (1) exhibits bi-stability in between the endemic equilibrium $E^*$ and the prey and disease free equilibrium $E_2$ for $\alpha \in (0.682543, 0.731164)$ depending on the initial consition, $\alpha = 0.731164$ system (1) shows another transcritical bifurcation. Beyond this point, as $\alpha$ increase the system (1) demonstrates multi-stability nature among $E_2$, $E_3$ and $E^*$ depending on initial condition. The system (1) also undergoes a hopf bifurcation at $\alpha = 0.782269$ in the disease free state $E_3$. For $\alpha \in (0.782269, 1.3168017)$ the system (1) again exhibits bi-stability in between $E_2$ and $E^*$. At $\alpha = 1.3168017$ system (1) exhibits a saddle-node bifurcation where two equilibrium points of opposite nature collide and vanish. For the higher value of $\alpha$ i.e., $\alpha > 1.3168017$

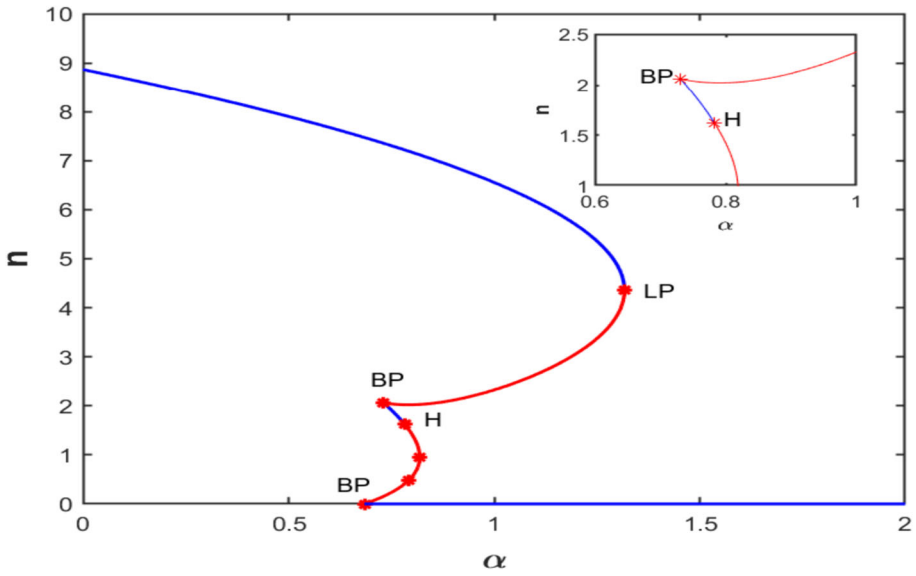


**Fig. 12** Bifurcation diagram with respect to the consumption rate $\alpha$

system (1) occurs only the prey and disease free state $E_2$ (see Fig. 12).

From the above discussion, it is very clear that the system (1) undergoes a very rich dynamical phenomena for the changes of parameter value $\alpha$. For relatively low consumption rate the prey population presence sufficiently to sustain the infected predator population, leading to a stable endemic state. As the consumption increase, the system experience qualitative changes in stability, moderate predation pressure can either suppress the disease or lead to extinction of predators if initial conditions are unfavorable. Further increase in consumption rate the system transit into multi-stability nature. This diversified outcomes leads to the complexity of predator prey interactions under intermediate ecological stress. At a certain point system undergoes hopf bifurcation, leading to oscillatory dynamics around the disease free state, higher predation stress prey and susceptible predator population fluctuate. Eventually as the consumption very high only the susceptible predator sustain.

#### 11.2.4 Role of prey refuge ($m$) in system dynamics

To study the role of proportional prey refuge of the system (1), we draw the bifurcation diagram with respect to the parameter $m$.

For low refuge $m$ the predator species get available favorite food resource that leads to the system (1) stable endemic state for $m < 0.772265$. At $m = 0.772265$ system (1) experienced a transcritical bifurcation. Further increase the value, system (1) shows bi-stability in between endemic ($E^*$) and disease free ($E_3$) stable state depends on the initial condition for $m \in (0.772265, 0.785088)$ and $m = 0.785088$ system (1) exhibits a saddle-node bifurcation where two equilibrium point of opposite nature collide and vanish. For higher value of $m > 0.785088$ system (1) shows only disease free ($E_3$) stable state (see Fig. 13).

From the above illustration, we observe that for lower prey refuge ($m$) helps to available sufficient amount of prey population for predator species that leads to endemic state. Higher refuge, impact on the availability of prey species as a result of this infected predator goes to the extinction and susceptible predator sustain due to alternating food resource. In addition moderate amount of refuge leads the system in a bi-stability nature depends on initial condition. Mondal et al. observed in their work lower value of refuge leads to the system oscillatory nature and higher value exhibits stable endemic state [10] this result disagree with our findings.

#### 11.2.5 Role of predator growth rate ($r_2$) in system dynamics

To study the role of predator growth rate ($r_2$), we draw a bifurcation diagram of the system (1) for prey species with respect to the predator growth rate $r_2$.

For low growth rate of predator species the system (1) shows unstable endemic state for $r_2 < 0.215529$, and the system (1) exhibits periodic oscillatory nature, as delineated by the red trajectory. For $r_2 = 0.215529$ system (1) experience a hopf bifurcation and for higher value of $r_2 > 0.215529$ system (1) shows stable endemic state (see Fig. 14).

From the numerical observation it is clear that, when the growth rate is relatively low, the system (1) failed to maintain a stable nature. In this case, the endemic equilibrium becomes unstable, and the population size exhibits oscillatory behavior over time. It creates a fragile ecological state, no such species sustain in a stable amount of values, due to the insufficient reproductive capacity of the predator species. At a critical threshold the system (1) undergoes a hopf bifurcation, which indicates a transition from unstable state to a

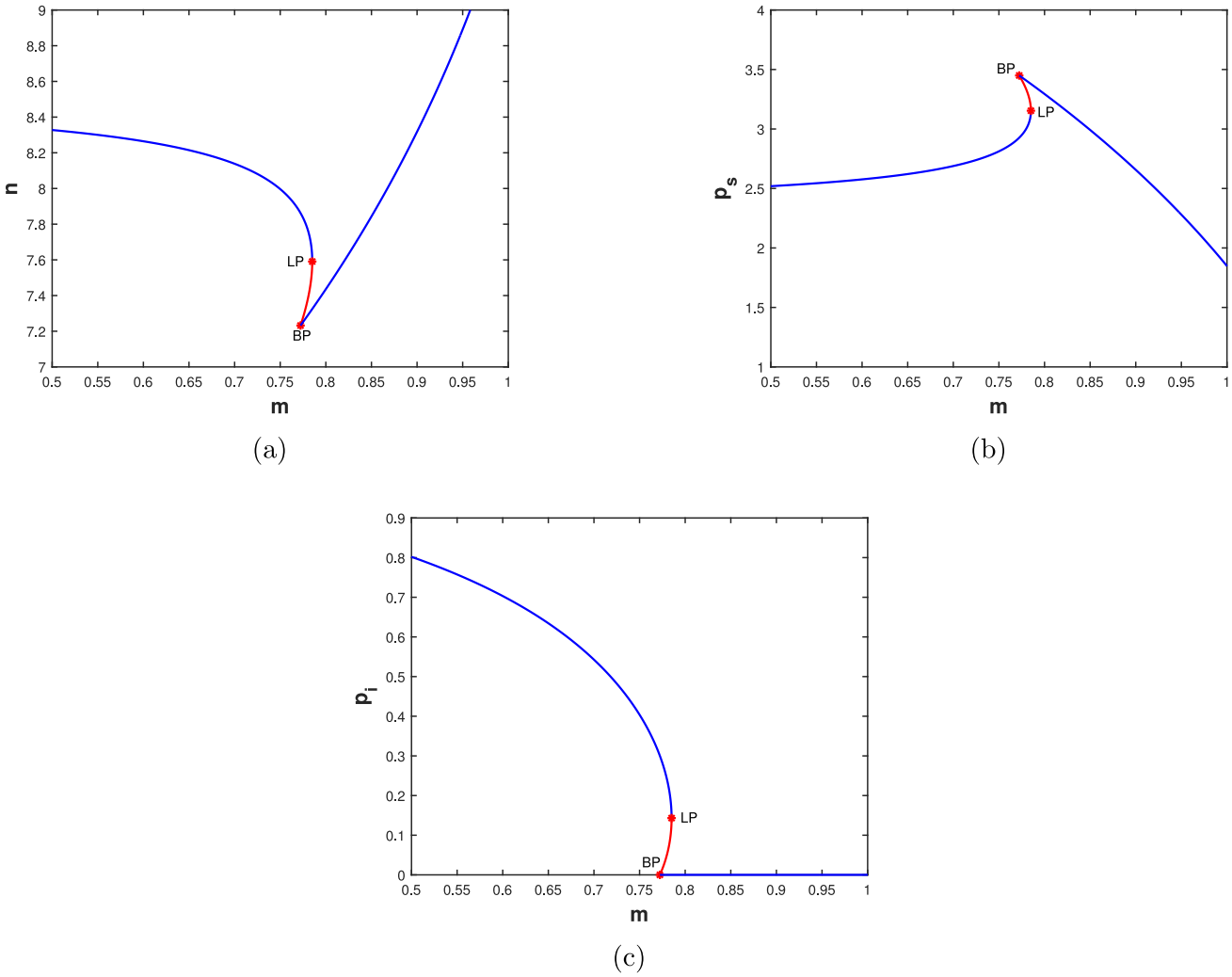


**Fig. 13** Bifurcation diagram with respect to the prey refuge $m$

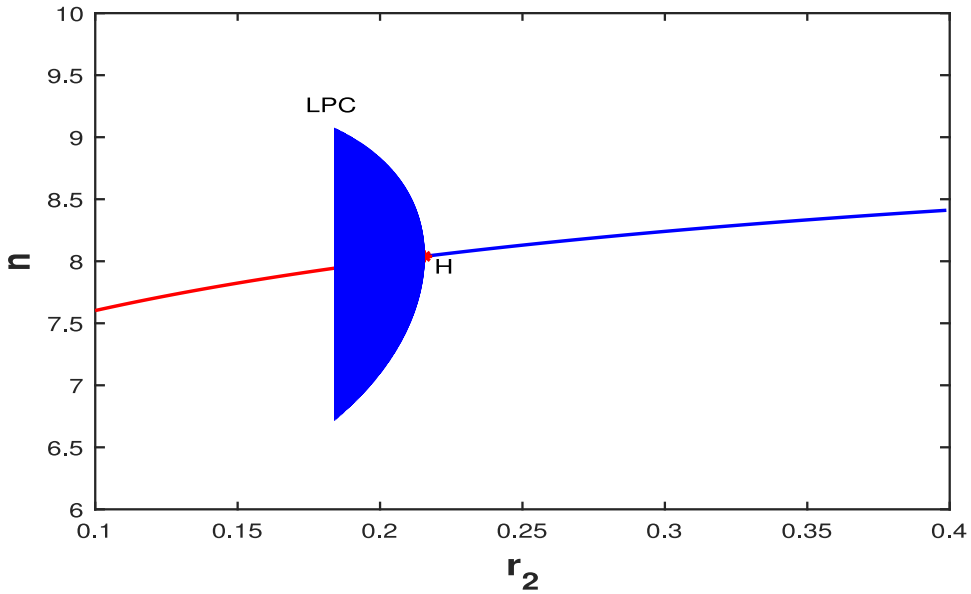


**Fig. 14** Bifurcation diagram of prey species with respect to the growth rate of predator species $r_2$

stable state. Beyond the threshold value system (1) stabilize in a endemic state in this regime the susceptible predator is robust enough to maintain the ecological balance, supporting both its own survival and support to persist the infected predator species also. This result differ with the findings of Pal [20] work, who demonstrated that lower predator growth leads to predator free stable state. However higher value shows the system unstable disease free state, contradict with our observation.

#### 11.2.6 Role of disease transmission rate ($e$) in system dynamics

To study the impact of disease transmission rate ($e$), we draw the bifurcation diagram of the system (1) with respect to the disease transmission rate ($e$). From the Fig. 15 it is clearly understood that for low disease transmission rate ($e < 0.228503$) system (1) undergoes disease free stable state $E_3$ and for $e = 0.228503$ the system (1) experience saddle-node bifurcation, where two equilibrium points of opposite nature collide and vanish. Further increase the value of $e$ system (1) shows bi-stability nature for the regime $e \in (0.228503, 0.259516)$. At $e = 0.259516$ the system experience a transcritical bifurcation, beyond the point $e > 0.259516$ system (1) shows stable endemic state $E^*$.

From the above discussion, we observed that lower amount of disease transmission supports to maintain disease free state. This happens because the infected predators are less effective for transmission of the infection to susceptible predators, limiting the spread of disease as well as allowing the susceptible predator population to persist with out being converted into the infected predator. Sha et al. showed that a lower disease transmission rate result in a disease free state, moderate value of disease transmission rate leads to occur coexisting state and higher value system showed susceptible predator free state [18]. Mondal et al. demonstrated in their work low disease transmission rate exhibits disease free oscillatory nature with higher amplitude, moderate value push the system endemic unstable state and the higher value system leads to the stable endemic state [10]. In contrast our results partially align with these findings [18] and [10] but also reveal important differences. Specifically, in a low disease transmission rate leading to the extinction of infected predator our observation agree with that status. As disease transmission rate increases, our result agree with the previous studies in showing a rise in infected species and little decline in susceptible predator. However, unlike [18] we observed in our study in high disease transmission rate, the prey population able to persist due to the collapse of susceptible predator population. Along with that our findings differ strongly with the observation of [10] for moderate value showed oscillatory endemic state but our result moderate amount of disease transmission leads a bi-stable nature in between stable disease free and endemic nature depends on the initial condition.

#### 11.2.7 Role of treatment ($\gamma$) in system dynamics

To study the role of treatment ($\gamma$), to draw a bifurcation diagram of the system (1) with respect to the treatment parameter $\gamma$.

For the low treatment rate $\gamma$ system (1) undergoes a stable endemic state $E^*$ for $\gamma \in (0, 1.074066)$. At $\gamma = 1.0474066$ the system (1) experienced transcritical bifurcation, which indicates to born new equilibrium point as a result of this the system (1) shows bi-stability for the regime $\gamma \in (1.074066, 1.634708)$ depends on the initial condition and $\gamma = 1.634708$ the system (1) exhibit saddle-node bifurcation where two equilibrium points of opposite nature collide and vanish. Beyond this point system (1) shows disease free stable nature $E_3$.

From Fig. 16 the above discussion we observe that, for low treatment rate infected predator are not effectively treated as a result, disease persist with in the predator species. In this case the system (1) stabilize an endemic state. As the treatment rate increases gradually and reaches to the threshold point, the system undergoes a trancritical bifurcation leading to the emergence of a new equilibrium. This makes a turning point where treatment begins a sensibly disrupt the cycle of transmission (susceptible to infected). The moderate treatment rates leads bi-stability nature. This reflects the ecological sensitivity to treatment effectiveness, moderate rate of treatment may or may not be able to eliminate the infection from the system (1) depends on the initial population size. For higher value of the treatment, the system structurally forced to moved into the disease free state, where only prey and susceptible predator sustain and infection is eradicated from the system (1). Mondal et al. showed in their work lower treatment rate leads to the system stable endemic nature slightly increment of treatment system undergoes a oscillatory endemic nature, further increase of treatment infected population vanished from the system where prey and susceptible predator showed oscillatory nature [10]. Our findings partially matched with their observation. Specifically for lower value and higher treatment value of treatment totally align with our findings. Moderate amount of treatment our system shows bi-stability nature which totally differ with [10].

#### 11.2.8 Effect of intra-species competition ($\nu$) and death rate of susceptible predator ($d_2$) in system dynamics

To study the effect of $\nu$ and $d_2$, we draw a bifurcation diagram of the system (1) with respect to the parameters $\nu$ and $d_2$ for prey species ($n$).

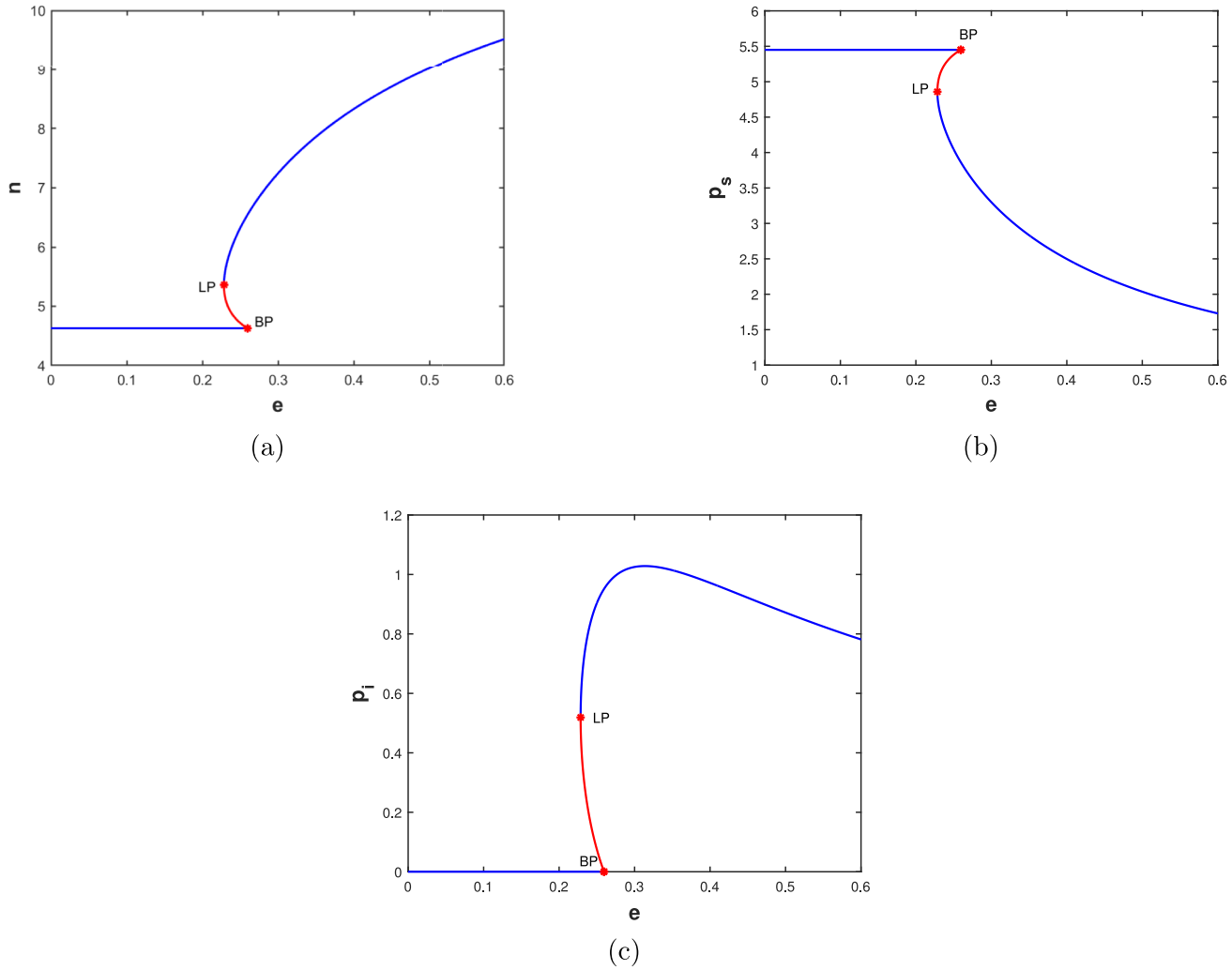


**Fig. 15** Bifurcation diagram with respect to the disease transmission rate $e$

For low value of $\nu$ the system (1) shows endemic state for $\nu < 0.4247962$, all species coexist in the system (1) with the stable nature where the healthy prey species presence in high amount. For $\nu = 0.4247962$ system (1) experience a transcritical bifurcation which introduced a new equilibrium state as a result the system shows bi-stability in the regime $\nu \in (0.4247962, 0.4632984)$ in between $E_3$ and $E^*$ depends on the initial condition. At $\nu = 0.4632984$ the system exhibits saddle-node bifurcation where two opposite nature equilibrium points collide and vanish. Beyond this point system undergoes disease free stable state ($E_3$) (see Fig. 17).

On the other hand system (1) maintain the stable endemic ($E^*$) state for low death rate $d_2 < 0.2173151$. At $d_2 = 0.2173151$ system (1) undergoes a transcritical bifurcation. As $d_2$ increase further system (1) shows disease free stable state ($E_3$) for $d_2 \in (0.2173151, 0.4)$, again the system (1) exhibits trancritical bifurcation at $d_2 = 0.4$ and beyond this point system (1) undergoes predator free stable state ($E_1$) (See Fig. 18). We have also summarized the above numerical observations of the systems (1) for different parameter values are in Table 2.

The bifurcation analysis established that system (1) exhibits bi-stability and multi-stability, under different parameter values. The trajectories are converging to distinct stable equilibrium states depending on the initial conditions. Figure 19a represents the phase portrait of bi-stability between $E_3$ and $E^*$ for the parameter value $f = 0.7$ and remaining parameter are taken from Table 1, corresponding to two different initial conditions. Figure 19b illustrates the phase portrait of bi-stability between $E_2$ and $E_3$ for the parameter value $r_1 = 0.73$, corresponding to two different initial conditions. Figure 19c presents the phase portrait of multi-stability among $E_2$, $E_3$ and $E^*$ for the parameter value $\alpha = 0.75$, corresponding to different initial conditions.

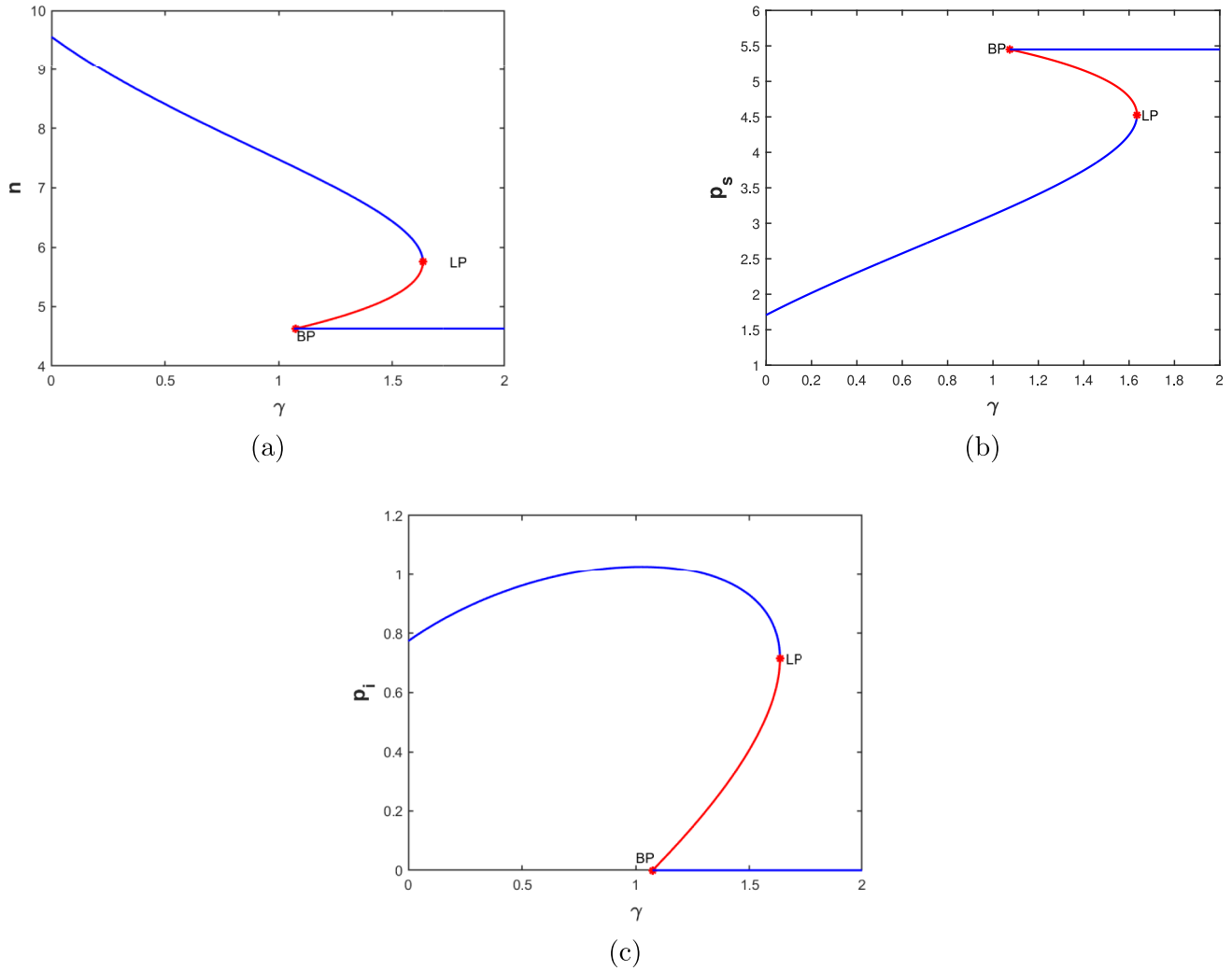


**Fig. 16** Bifurcation diagram with respect to the treatment parameter $\gamma$

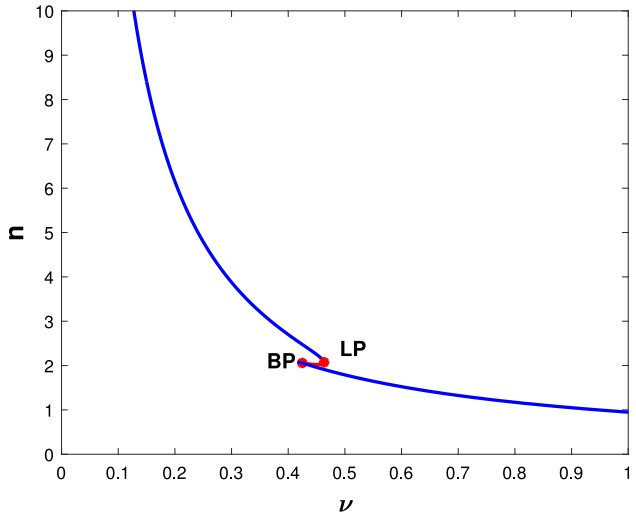


**Fig. 17** Bifurcation diagram with respect to the intra-species competition ($\nu$)

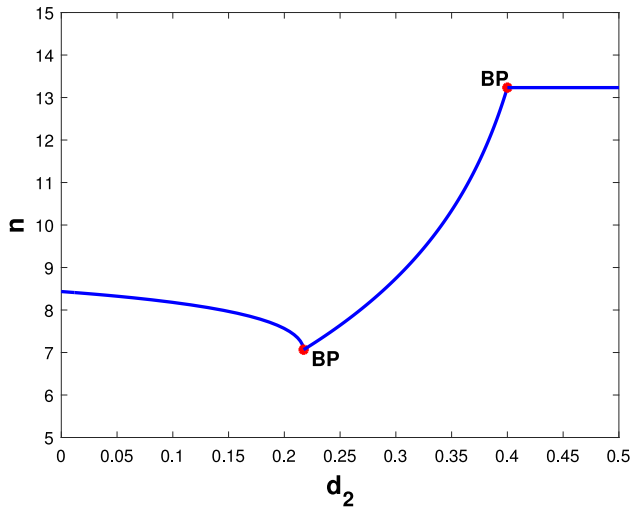


**Fig. 18** Bifurcation diagram with respect to the natural death rate of susceptible predator ($d_2$)

**Table 2** Parameter ranges and dynamics of the system (1)

| Parameter | Range | Dynamics/Nature |
|---|---|---|
| $r_1$ | (0 – 0.7120009) | Stable prey and disease free state ($E_2$) |
| | (0.7120009–0.743567824) | Bi-stability in between $E_2$ and $E_3$ |
| | (0.743567824–0.9297507) | Stable disease free state ($E_3$) |
| | (0.9297507–1.0439525) | Bi-stability in between $E_3$ and $E^*$ |
| | (1.0439525–2) | Stable endemic state ($E^*$) |
| $f$ | (0-0.6486475) | Stable endemic state ($E^*$) |
| | (0.6486475 – 0.8317018) | Bi-stability in between $E_3$ and $E^*$ |
| | (0.8317018–1.4524291) | Stable disease free state ($E_3$) |
| | (1.4524291–1.4638723) | Bi-stability in between $E_3$ and $E_2$ |
| | (1.4638723–2) | Stable prey and disease free state ($E_2$) |
| $\alpha$ | (0 – 0.682543) | Stable endemic state ($E^*$) |
| | (0.682543 – 0.731164) | Bi-stability in between $E_2$ and $E^*$ |
| | (0.731164–0.782269) | Multi-stability among $E_2$, $E_3$ and $E^*$ |
| | (0.782269–1.3168017) | Bi-stability in between $E_2$ and $E^*$ |
| | (1.3168017–2) | Stable prey and disease free state ($E_2$) |
| $m$ | (0 – 0.772265) | Stable endemic state ($E^*$) |
| | (0.772265 – 0.785088) | Bi-stability in between $E_3$ and $E^*$ |
| | (0.785088–1) | Stable disease free state ($E_3$) |
| $r_2$ | (0.1–0.215529) | Oscillatory endemic state ($E^*$) |
| | (0.215529–0.4) | Stable endemic state ($E^*$) |
| $e$ | (0–0.2228503) | Stable disease free state ($E_3$) |
| | (0.2228503 – 0.259516) | Bi-stability in between $E_3$ and $E^*$ |
| | (0.259516–0.6) | Stable endemic state ($E^*$) |
| $\gamma$ | (0–1.074066) | Stable endemic state ($E^*$) |
| | (1.074066 –1.634708) | Bi-stability in between $E_3$ and $E^*$ |
| | (1.634708–2) | Stable disease free state ($E_3$) |
| $v$ | (0–0.424796) | Stable endemic state ($E^*$) |
| | (0.4247962–0.4632984) | Bi-stability in between $E_3$ and $E^*$ |
| | (0.4632984–1) | Stable disease free state ($E_3$) |
| $d_2$ | (0–0.2173151) | Stable endemic state ($E^*$) |
| | (0.2173151 –0.4) | Stable disease free state ($E_3$) |
| | (0.4–0.5) | Stable predator free state ($E_1$) |

Ecologically, these findings imply that the system can settle into different stable community states under the same environmental and parametric conditions, solely determined by the initial population distribution. The observed bi-stability indicates the potential coexistence of two alternative stable states for instance, a disease free healthy coexistence state and a predator dominant state whereas multi-stability reflects the possibility of multiple alternative equilibria. Such phenomena highlight the sensitivity of ecological communities to initial population levels and suggest that small perturbations may drive the system toward entirely different long term outcomes, which is highly relevant in ecosystem management and conservation.

### 11.3 Contour representation of the species biomass effect of two different parameters

In this section we study the density of the species for changes of selected parameter and the other parameters values taken from the Table 1. Axis are represented by the parameter and the color is evaluate the biomass of the particular species which represented by the color line. In Fig 20a horizontal axis

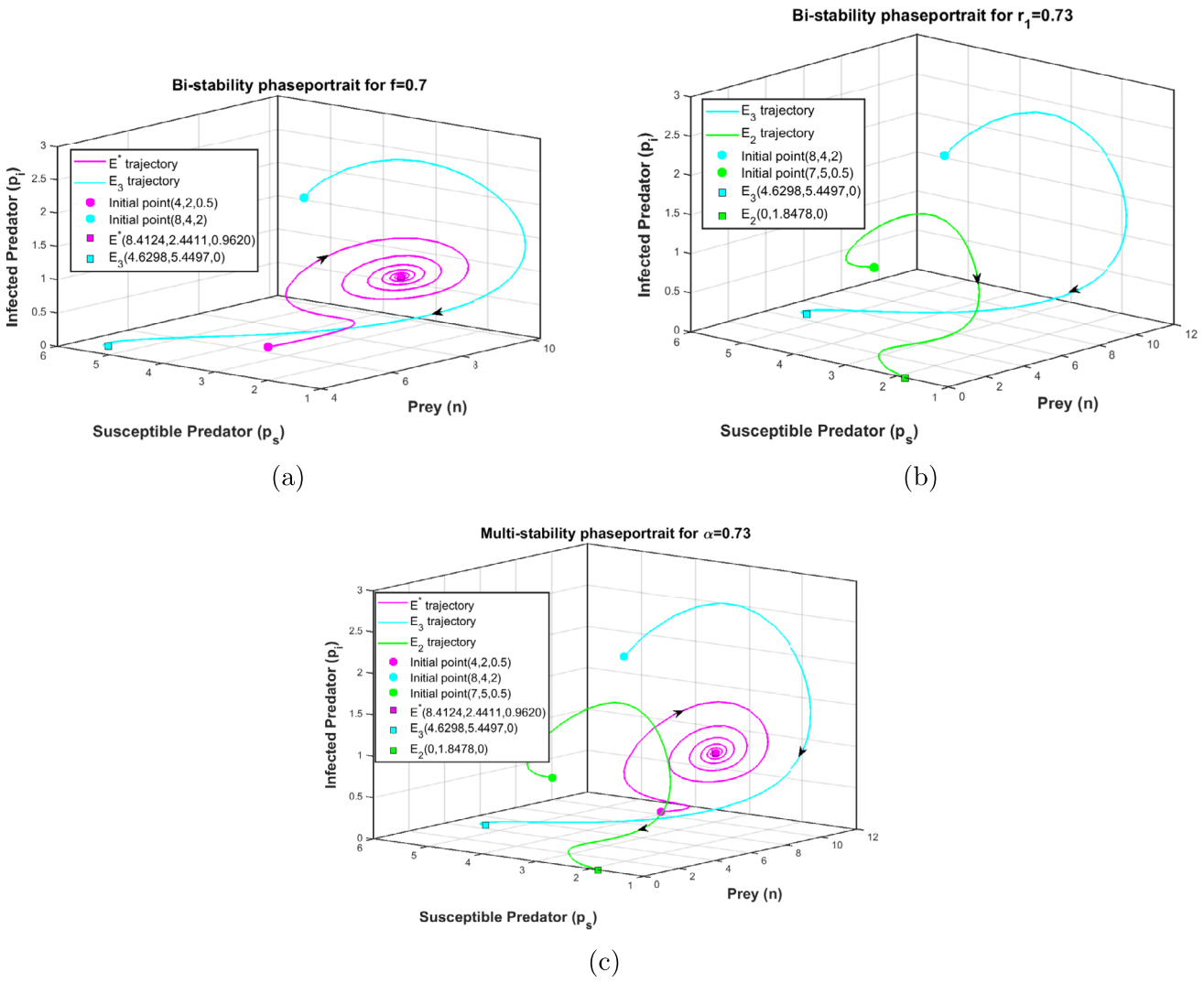


**Fig. 19** Phase portrait of bi-stability and multi-stability

represents the prey refuge ($m$) and the vertical axis represents the alternating food resources ($\eta$) for susceptible predator, changes of the parametric value how effective in the biomass of susceptible predator ($p_s$) measure by the color mention in the color line. For low value of $m$ maintain the reasonable amount of susceptible predator, moderate level of refuge helps to maintain high level of predator density and the high value of $m$ along with small value of $\eta$ decrease the susceptible predator density. In Fig 20b, c horizontal axis represents the disease transmission rate ($e$) and vertical axis represents the treatment ($\gamma$), Fig 20b measure the biomass of susceptible predator and 20c biomass of infected predator. Low values $e$ helps to increase the susceptible predator density whereas decrease the infected predator density. Higher value of $e$ and the lower value of $\gamma$ gradually tends to low density of susceptible predator and high density of infected predator. Higher value of $e$ also able to maintain the infected predator density in presence of high treatment rate. In Fig 20d horizontal axis represents the growth rate ($r_2$) of susceptible predator and vertical axis represents the disease transmission rate ($e$). The high level of $e$ decrease the density of susceptible predator and low level of $e$ maintain the high density of susceptible predator for any value of $r_2$.

## 11.4 Two parameters bifurcation

To know the behavior of system (1) in more deeper and illustrative way, we study two parameters bifurcation, where we varies two selected parameters and the other parameter values consider from the Table 1. We draw the stability regions of the equilibrium points $E_2$, $E_3$ and $E^*$ respectively. In the region plots Figs. (21, 22, 23 and 24) blue colored line represents the BP (transcritical bifurcation) curve, the red line represenst the LP (saddle-node bifurcation) curve and the

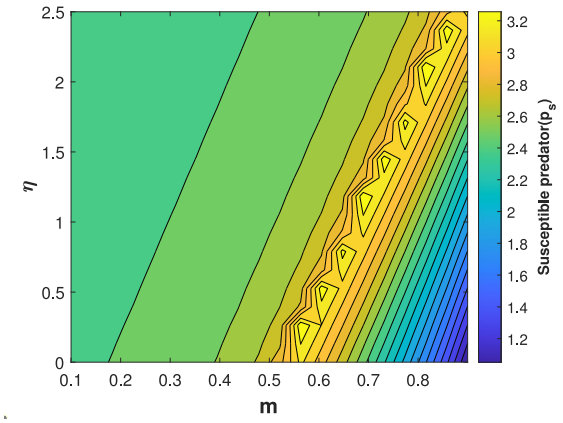


(a) Contour diagram $\eta$ and $m$ to measure the biomass of susceptible predator species.

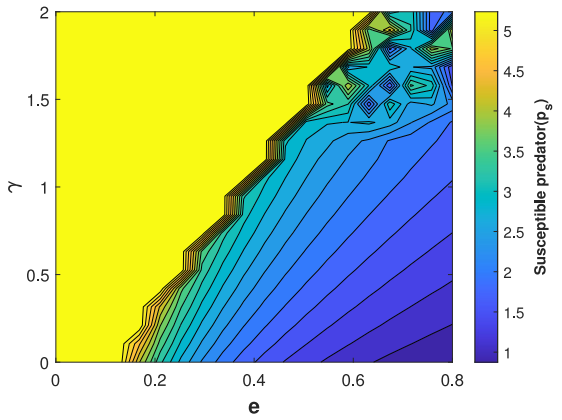


(b) Contour diagram $e$ and $\gamma$ to measure the biomass of susceptible predator species.

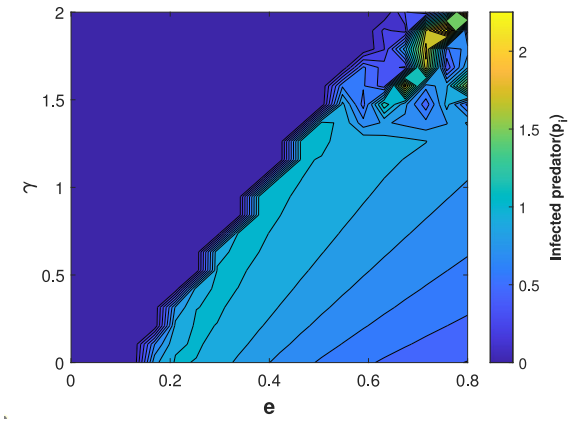


(c) Contour diagram $e$ and $\gamma$ to measure the biomass of infected predator species.

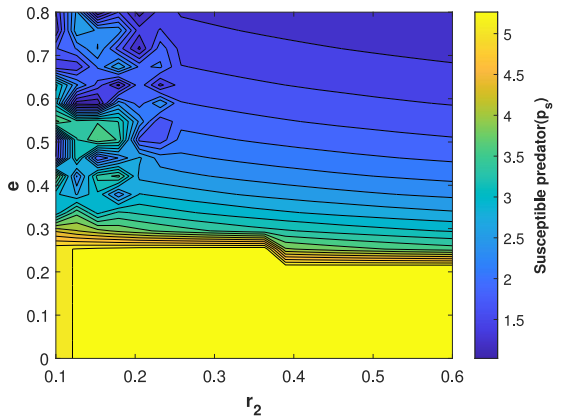


(d) Contour diagram $e$ and $r_2$ to measure the biomass of susceptible predator species.

**Fig. 20** Contour diagram

green line represents the H (hopf bifurcation) curve. The yellow shaded region ($R_1$) represents the stability region of the endemic equilibrium $E^*$, the orange shaded region ($R_2$) corresponds to the bi-stable region in between infection free $E_3$ and endemic $E^*$ stable state, the turquoise shaded region ($R_3$) indicates the stability region of the infection free equilibrium $E_3$, the pink shaded region ($R_4$) represents the bi-stability in between two stable state $E_3$ and $E_2$, the lime shaded region ($R_5$) indicates prey and infection free $E_2$ stable state, the rose shaded region ($R_6$) indicates bi-stability in between two stable regions $E^*$ and $E_2$, the brown shaded region ($R_7$) indicates the multi-stability where three stable states occur $E_2$, $E_3$ and $E^*$ and the lavender shaded region ($R_8$) indicates the unstable endemic state.

From Fig. 21, its observed that small value $f(< 0.6)$ the system (1) maintain the stable endemic state in the region $R_1$ for the value of $m(< 0.87)$, increase the value of $f$ specifically, $f \in (0.6, 0.85)$, the infected predator population gradually decrease due to the fear effect make an impact on prey species create shortage of food source may leads to extinction the infected predator population, the result of this, region $R_2$ represents the bi-stability. For any value of $m$ along with $f \in (0.85, 1.15)$ leads the system totally infection free due to the increment of fear in the region $R_3$. Further increase of fear and low level of prey refuge ($m < 0.21$) makes the system (1) bi-stable where infection free state ($E_3$) and prey and infection free state ($E_2$) coexist in the region $R_4$ and the high value of fear and low refuge leads to the system (1) prey and disease free.

Fig 22 illustrates the complex dynamical nature of system (1). A low consumption rate ($\alpha$) supports the persistence of both prey species and the infected predators, allowing the system to maintain stable endemic state represented in the region $R_1$. The moderate level of refuge $m \in (0.6, 0.63)$ and high amount of consumption rate $\alpha > 1.3$ indicates the system (1) may transition to an infection free state depending on

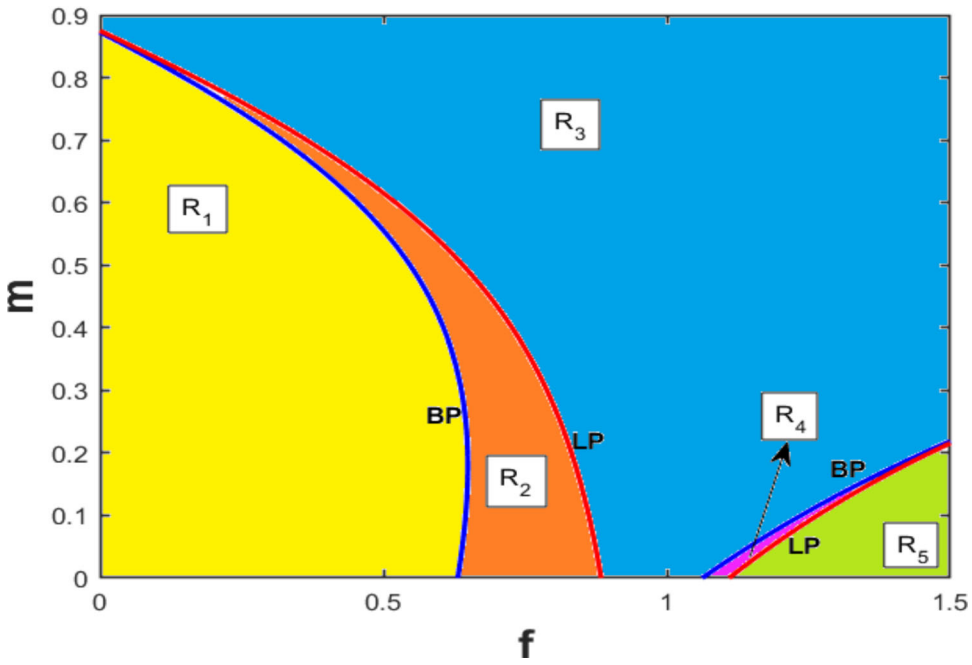


**Fig. 21** Domains of stability and instability of the system (1) in $f$–$m$ parameter space where other parameter values are taken from Table 1. The horizontal axis represents the fear effect $f$ and the vertical axis represents refuge of prey species $m$. The yellow region $R_1$ depicts that endemic equilibrium point $E^*$ is stable, the orange region $R_2$ depicts bi-stable region in between disease free stable state $E_3$ and stable endemic state $E^*$, the turquoise region $R_3$ depicts infection free equilibrium $E_3$ is stable, the pink region $R_4$ depicts bi-stability in between infection free $E_3$ and prey and infection free $E_2$ stable state and the lime region $R_5$ depicts prey and infection free $E_2$ stable state. (Color figure online)

the initial condition. This scenario gives rise to a bi-stability denoted in the region $R_2$. A High value of refuge $m$ derives the system (1) towards infection free state regardless any value of $\alpha$ as represented the region $R_3$. A moderate value of consumption rate $\alpha$ leads the system (1) bi-stability in between stable endemic and stable prey and disease free states, indicates in the region $R_6$. Region $R_7$ exhibits three coexisting stable equilibrium state $E_2$, $E_3$ and $E^*$ for $(m < 0.4)$ depending on the initial condition of the system (1). Finally, a high value of $\alpha$ with $m < 0.6$ derives the system (1) toward a prey and infection free state, represented in the region $R_5$.

Figure 23 describes the two parameter bifurcation, for the low growth rate of susceptible predator $r_2$ and the high value of disease transmission rate $e$ system (1) shows unstable endemic state, represented in the region $R_8$. For low growth rate of susceptible predator and low disease transmission rate along with high disease transmission rate and high growth rate of susceptible predator leads the system endemic stable state, represented in the region $R_1$.

From Fig 24, it is observed that low disease transmission rate regardless of the treatment rate leads to extinction of infected predator population and derives the system (1) towards a stable infection free state, represented by region $R_3$. In contrast, a higher disease transmission rate supports the persistence of the infected predator species, resulting in a stable endemic state for the system (1), as represented by region $R_1$.

## 11.5 Global stability

In this section, we numerically study the global stability of three vital equilibrium points; interior $(E^*)$, disease free $(E_3)$ and prey and disease free $(E_2)$ of the system (1). First, we examine the global dynamics of the interior equilibrium $(E^*)$. For the parameter values given in Table 1, we have four feasible equilibria $E_1(13.2333, 0, 0)$, $E_2(0, 1.8478, 0)$, $E_3(4.6298, 5.4497, 0)$ and $E^*(8.4124, 2.4411, 0.9620)$. At $E_1$ eigenvalues are $-1.9850$, $0.3890$, $-1.4143$, at $E_2$ eigenvalues are $-0.3890$, $0.9174$, $-0.6567$, at $E_3$ eigenvalues are $-0.4377 \pm 0.4354i$, $0.8201$, and at $E^*$ eigenvalues are $-0.0475 \pm 0.5526i$, $-1.1637$. Hence only one interior equilibrium exist and stable in nature, whereas the remaining feasible equilibria are unstable. So all solution trajectories converge to this equilibrium point from various positive initial conditions, indicating global asymptotic stability of $E^*$ for the parameter values mentioned in Table 1 (see Fig. 25).

We further observe that the system (1) is globally asymptotically stable around the disease-free fixed point $(E_3)$ for $\beta = 0.2$, where other parameter values are remain unchanged as in Table 1 (see Fig. 26). The system (1) possesses five feasible different equilibrium points, namely $E_1(13.2333, 0, 0)$, $E_2(0, 1.847750, 0)$, $E_3(4.6298, 5.4497, 0)$, $E^*(8.015, 2.721, 1.0031)$ and $E^*(4.7954, 5.3187, 0.1377)$. The eigenvalues associated with these equilibria as follows: for $E_1(13.2333, 0, 0)$: $-1.9850$, $0.3890$, $-3.20$; for $E_2$ $(0, 1.8478, 0)$: $-0.3890$, $0.9174$, $-2.4424$; for $E_3(4.6298, 5.4497, 0)$: $-0.4377 \pm 0.4354i$,$-0.9656$; for $E^*(8.015, 2.721, 1.0031)$: $-1.0832$, $0.0068 \pm 0.5743i$; and for $E^*$

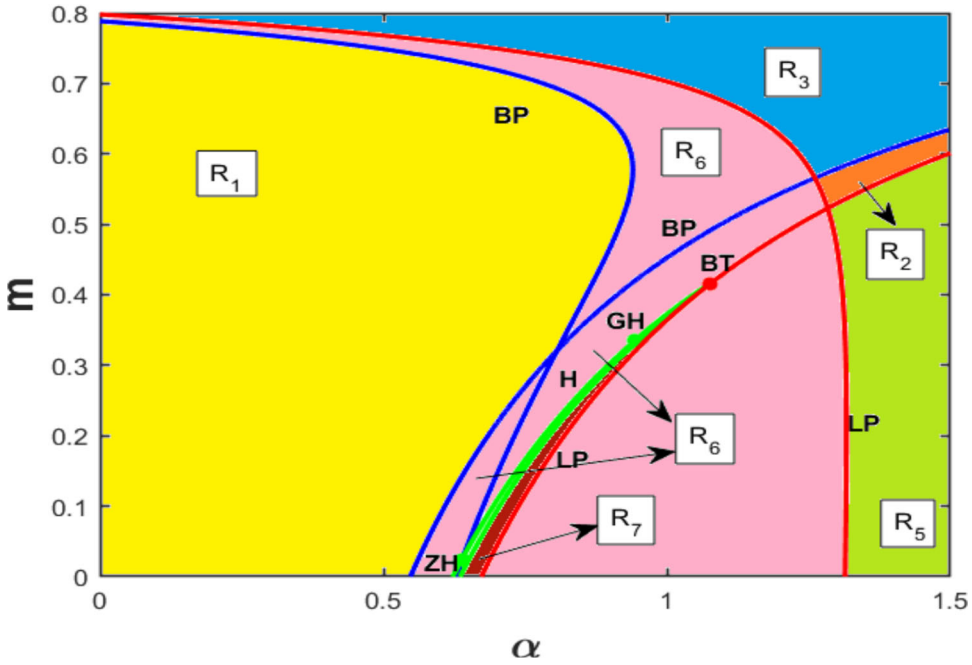


**Fig. 22** Domains of stability and instability of the system (1) in $\alpha$–$m$ parameter space where other parameter values are taken from Table 1. The horizontal axis represents the consumption rate $\alpha$ and the vertical axis represents refuge of prey species $m$. The yellow region $R_1$ depicts that endemic equilibrium point $E^*$ is stable, the orange region $R_2$ depicts bi-stable region in between disease free stable state $E_3$ and stable endemic state $E^*$, the turquoise region $R_3$ depicts infection free equilibrium $E_3$ is stable, the lime region $R_5$ depicts prey and infection free $E_2$ stable state, the rose region $R_6$ depicts bi-stability in between $E_2$ and $E^*$ stable state and the brown region $R_7$ depicts the multi-stability in between $E_2$, $E_3$ and $E^*$

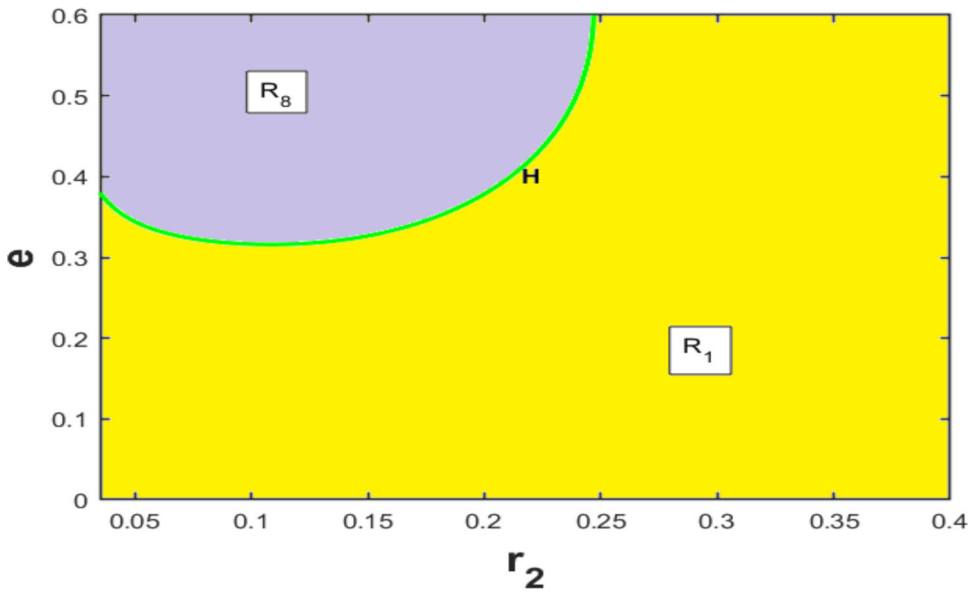


**Fig. 23** Domains of stability and instability of the system (1) in $r_2$–$e$ parameter space where other parameter values are taken from Table 1. The horizontal axis represents the growth rate of susceptible predator $r_2$ and the vertical axis represents disease transmission rate $e$. The yellow region $R_1$ depicts that endemic equilibrium point $E^*$ is stable and the lavender region $R_8$ depicts unstable endemic state.(Color figure online)

(4.7954, 5.3187, 0.1377): are $-0.4320 \pm 0.4305i$, 0.5378. Thus, the unique equilibrium $E_3$ is feasible as well as stable, where as remaining equilibria are not stable in nature. For different initial values, all the trajectories converges to unique equilibrium $E_3$ (see Fig. 26).

The system (1) admits two feasible equilibria, $E_1$ (13.2333, 0, 0) and $E_2$(0, 1.8478, 0) for $f = 1.5$ and the other parameter values taken from Table (1). The eigenvalues corresponding to $E_1$ are $-1.9850$, 0.3890, and $-1.4143$, while those associated with $E_2$ are $-0.3890$, $-0.0127$, $-0.6567$. Hence the unique equilibrium $E_2$ is feasible and stable, whereas the $E_1$ is unstable in nature. For different initial values, all the trajectories converge to unique equilibrium $E_2$ (see Fig. 27). Therefore, the system is globally asymptotically stable around the equilibrium $E_2$ for the given set of parameter values.

### 11.6 Optimal control analysis

To solve the optimality associated with the system (1) numerically, the forward backward sweep method is employed. In this approach, the system of adjoint equations is solved backward in time, and in each iteration, the control variable $\gamma$ is updated based on the current state and adjoint trajectories. The process is repeated iteratively until the solution converges within a desired tolerance.

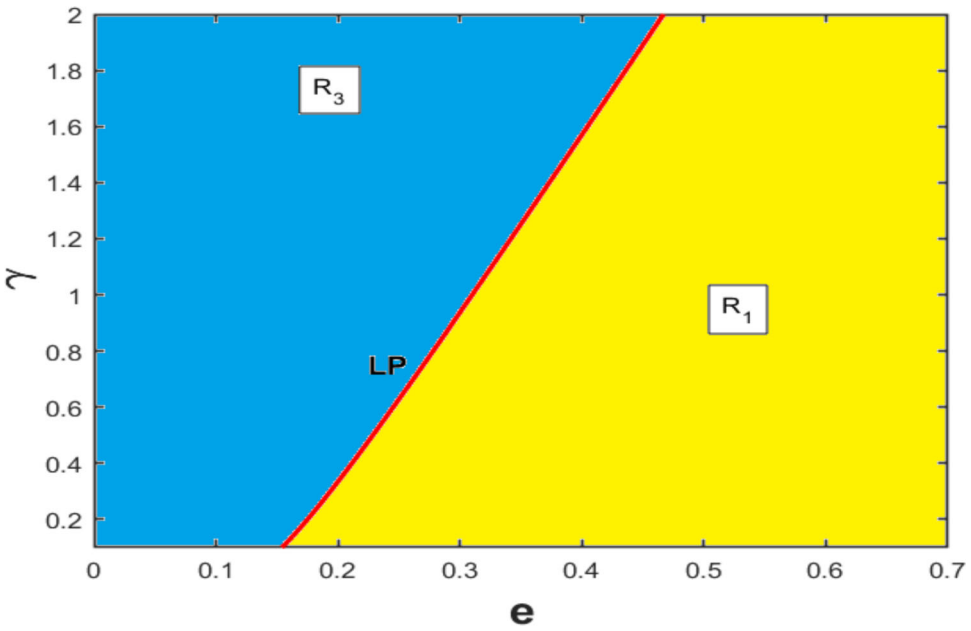


**Fig. 24** Domains of stability and instability of the system (1) in $e$–$\gamma$ parameter space where other parameter values are taken from Table 1. The horizontal axis represents the disease transmission rate $r_2$ and the vertical axis represents the treatment $\gamma$. The yellow region $R_1$ depicts that endemic equilibrium point $E^*$ is stable and the turquoise region $R_3$ depicts the infection free stable state.(Color figure online)

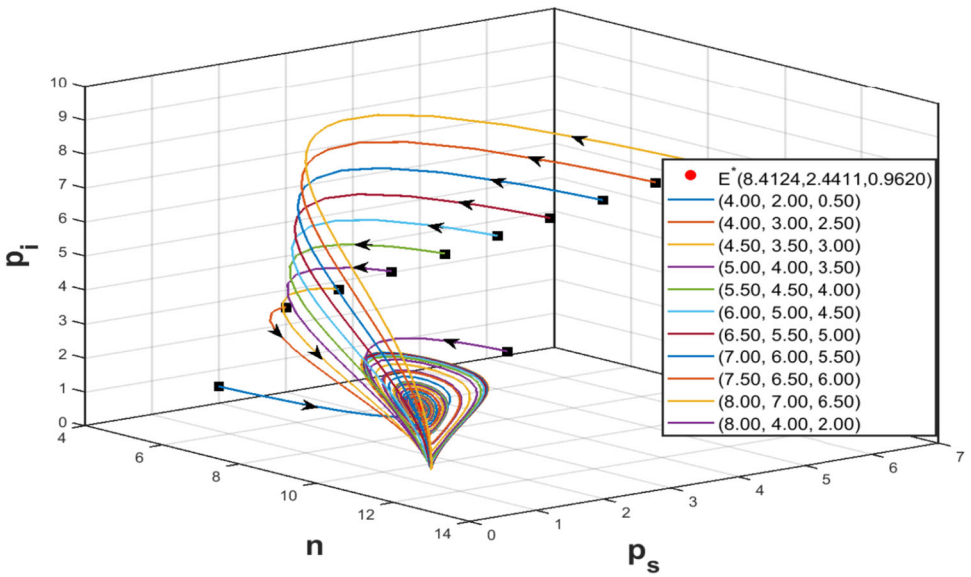


**Fig. 25** The figure express the global stability of the model system (1) at the equilibrium point $E^*(8.4124, 2.4411, 0.9620)$ for the parametric values specified in Table 1

For the simulation, the weight factors in the cost functional are chosen as $\xi = 1.7$ for the infected predator biomass and $\phi = 2$ for the treatment effort. All other model parameters value are taken from Table 1 and the initial population sizes are consider as $n = 4.0$, $p_s = 2.0$ and $p_i = 0.5$ respectively. The simulation is carried out over the time frame [0, 500].

Figure 28a, b and c illustrates the comparative dynamics of the prey, susceptible predator and infected predator populations with and without control. It is evident from the figure that the application of the time dependent optimal control results in a significant reduction in the infected predator population and a corresponding increase in the susceptible predator population.

Figures 28d and e represent the optimal control profile along with the transversality condition $\psi_i(T) = 0$, $i = 1(1)3$. It's observed that the optimal strategy involves applying the maximum treatment effort up to approximately 240.74 units of time, after which the control effort is gradually reduced. As time progresses, the adjoint variable associated with the infected predator denoted as $\psi_i(t)$ approaches to zero. This behavioral phenomenon satisfying the transversality condition $\psi_i(T) = 0$. It is the necessary boundary condition derived from Pontryagin's Maximum principal. The results replicate that the optimal treatment strategy is highly effective in reducing the number of infected predators and can ultimately eradicate the infection from system (1).

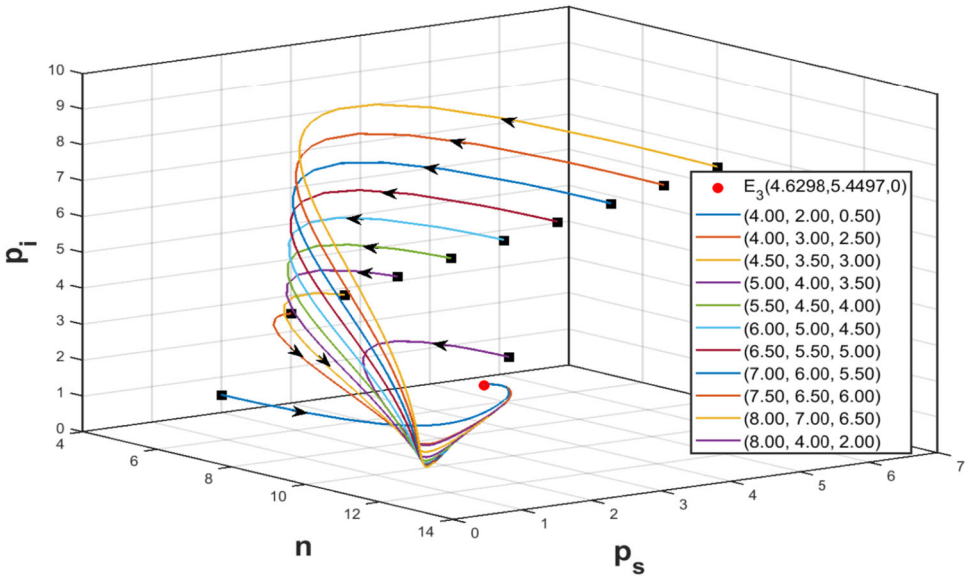


**Fig. 26** The figure express the global stability of the model system (1) at the equilibrium point $E_3(4.6298, 5.4497, 0)$ for $\beta = 0.2$ and other parametric values are given from Table 1

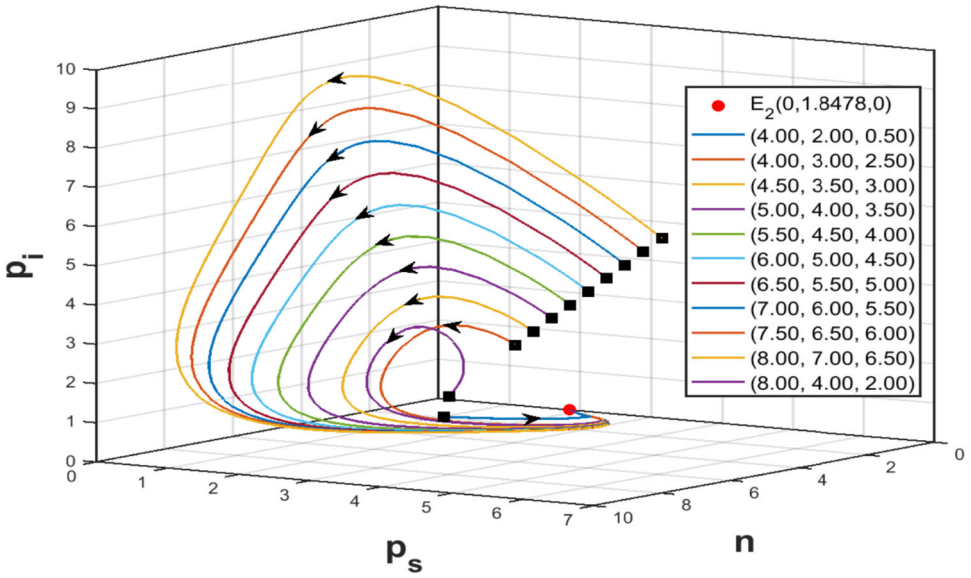


**Fig. 27** "The figure express the global stability of the model system (1) at the equilibrium point $E_2(0, 1.8478, 0)$ for $f = 1.5$ and other parametric values are given from Table 1

## 12 Discussion and conclusion

Classical eco-epidemic model are studied by many authors over the past few decades, since the pioneering work [11] to get a better insight. Researchers are gradually incorporating several phenomena like fear effect [1, 18, 27], using modified Leslie-Gower model to provided additional food resources [19, 20, 31], some of the researcher are integrated prey proportional refuge to protect prey species from predation [10, 37] and recently Mondal et al. [10] assimilate treatment for infected predator species. In the present investigation, we incorporate many biological phenomenon like fear, refuge, alternating food resources and treatment for disease effected species on our model. Summarizing the analytical results along with that support of numerical evidence, the proposed system (1) exhibited four biologically viable equilibrium points. The first equilibrium point (only prey species exist) $E_1$ exist if $r_1 > d_1$ and it is stable when $r_2 < d_2$. The second equilibrium point $E_2$ (where the susceptible predator exist) stable when $E_1$ is unstable. The third equilibrium point $E_3$ which is disease free state exist and stable under the condition $\mathcal{R}_0 < 1$, provided $u_{11}^{[3]} + u_{22}^{[3]} < 0$ and $u_{11}^{[3]}u_{22}^{[3]} - u_{12}^{[3]}u_{21}^{[3]} > 0$. Finally, the last equilibrium point $E^*$ where all three species coexist and the equilibrium point is stable under Routh-Hurwitz criterion. We consider Lyapunov function to prove global behavior, the system (1) is globally asymptotically stable around the equilibrium point $E_2$ if it exists. To establish the global stability of $E_3$ analytically we use Bendixson-Dulac criterion. The endemic equilibrium point global stability established by using suit-

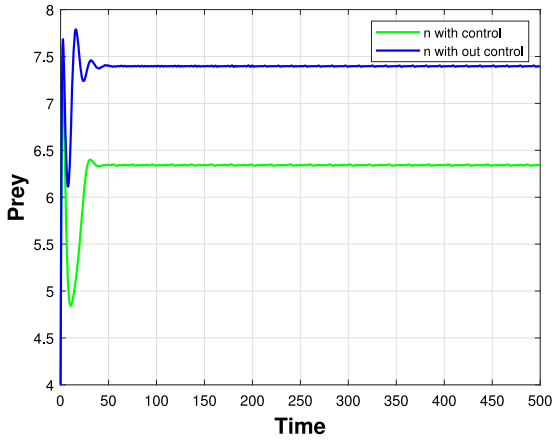


(a)

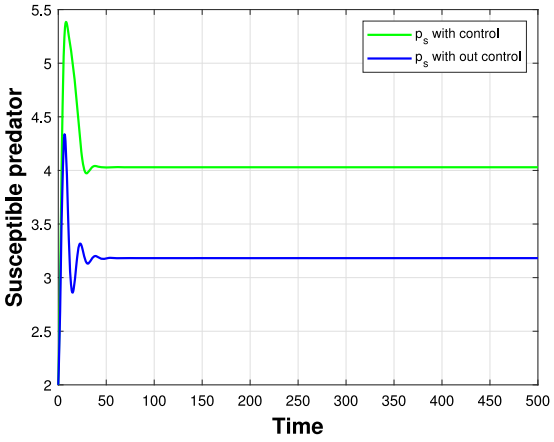


(b)

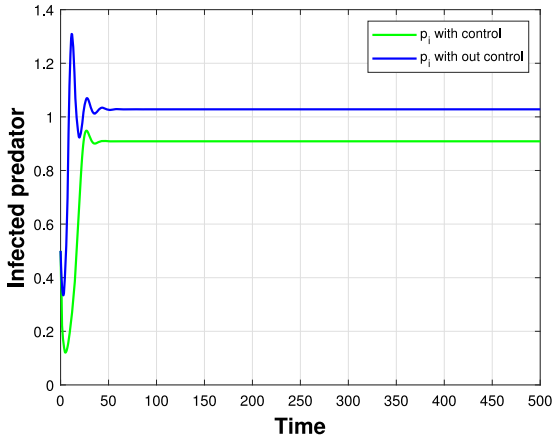


(c)

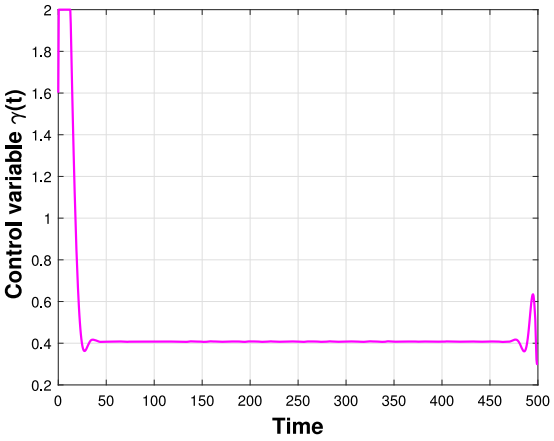


(d)

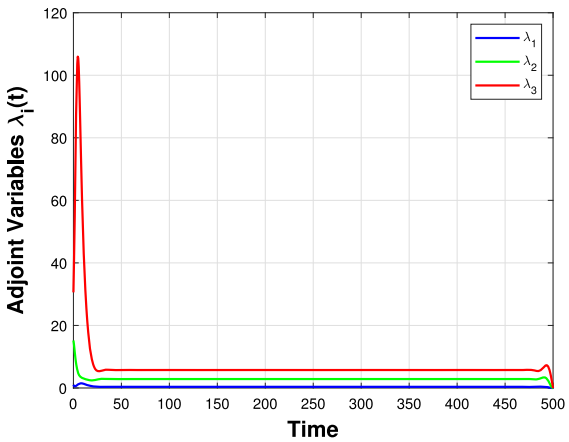


(e)

**Fig. 28** Time series representation of each population with and without control (**a**, **b**, **c**); control variable($\gamma$) represent (**d**); (**e**) represents the adjoint variables ($\lambda_i$). Parameters are at the same values as in Table 1. Moreover, we take $\xi = 1.7$ and $\phi = 2$

able positive definite function. The system (1) experienced a transcritical bifurcation at $r_1 = r_1^{[TC_2]}$, where $r_1^{[TC_2]} = \left(\frac{d_1}{r_2} + \frac{\alpha(1-m)(r_2-d_2)\eta}{ar_2^2}\right)(r_2 + f(r_2 - d_2)\eta)$ around prey and disease free equilibrium point $E_2$. The boundary equilibrium point $E_3$ of the system (1) shows saddle-node bifurcation at $r_1 = r_1^{[SN]}$, transcritical bifurcation at $e = e^{[TC_1]}$, where $e^{[TC_1]} = \frac{\beta d_3 + \gamma}{e\beta}$ and Hopf bifurcation at $\alpha = \alpha^{[HB_1]}$. In addition the system (1) undergoes a Hopf bifurcation around $E^*$ at $r_2 = r_2^*$.

In this context, we studied comprehensive numerical simulation to unveiling the intricate behavior of the proposed model system (1). For this numerical study we considered set of parametric value mentioned in Table 1. Primarily we investigated the sensitive parameter for infected predator biomass using PRCC technique, it is observed that the disease transmission rate $e$, death rate of prey $d_1$ are most positive sensitive parameter, gradually increase of those parameters value helps to increase the infected predator biomass (see Fig. 1). Along with that to study the strength of the parameter we generated PRCC violin plot (see Fig. 2), where the consumption rate $\alpha$, disease transmission rate $e$, treatment delay $\beta$ and death rate of infected predator $d_3$ are the strengthen parameters to influence in infected predator biomass. Further study of the normalized sensitivity to judge which parameter influence to increase the reproduction number, we observed that the disease transmission rate $e$ is positively sensitive in that case (see Fig. 3). In Fig. 4 we showed that measure of the reproduction number for changes of two parameters and susceptible predator biomass. System (1) experienced decline of prey biomass due to gradually increase of fear and goes to the extinction for $f = 1.6$ with the presence of very low refuge at $m = 0.2$ (see Fig. 5). For the same amount of fear the prey species protected form extinction due to the increase of prey refuge, for $m = 0.6$ the prey species $n(t) = 1.58$ (see Fig. 6) and $m = 0.8$ the prey species $n(t) = 2.15$ (see Fig. 7). The contour diagram express the biomass of prey species with the varying of two parameter simultaneously (see Fig. 9). In addition the system showed slightly downfall of prey biomass for sensible amount of intra-species competition and system (1) growing in a constant rate up to the threshold value then its growing exponentiation for very low amount of intra-species competition (see Fig. 8).

Among all parameters, some directly influence the demographic changes of the proposed system (1). We interpreted the changes using bifurcation study, the growth rate of prey species ($r_1$), fear effect ($f$), consumption rate of predator species ($\alpha$), prey refuge ($m$), predator growth rate ($r_2$), disease transmission rate ($e$) and the treatment effect ($\gamma$). We observed that the system (1) showed a stable endemic state for high value of $r_1$, because of sufficient food availability for predator and prey refuge able to protect prey species. Slightly low value of $r_1$ reflect bi-stability in between endemic and disease free state due to food deficiency of infected predator. The system showed disease free nature when decrease again the growth rate. Along with that the system (1) may occurred another bi-stability to reduce more the value of $r_1$, which depends on initial condition. In addition for lower growth rate system (1) only persist the susceptible predator depends on the additional food resources (see Fig. 10). Our observation align with the work of Mondal et al. [10] for higher growth rate but for low growth rate system showed disease free up to a certain threshold value then oscillatory disease free state, which differ from our observation. For very high values of the fear effect ($f$), only the susceptible predator population can sustain due to alternating food source. At slightly lower fear levels, the system (1) undergoes an bi-stability, where both $E_2$ and $E_3$ are possible, depending on the initial conditions. For moderate amount of fear the system (1) leaned towards disease free state, as the fear effect on the prey population causes a downfall in prey population, which leads to the system (1) move towards disease free state. Low levels of fear helps to persist the prey species in the system (1) maintains a stable endemic state. Mondal et al. observed that changing the value of fear lower to higher system exhibits a stable endemic nature to an oscillatory disease free state to disease free stable state [10] which partially align with our result. However Sarkar et al. demonstrated that in their work an increase in fear did not effect significantly in the growth of prey species [32] this result contradict of our findings.

For low consumption rates, the prey population remains sufficiently abundant to sustain the infected predator population, resulting in a stable endemic state. As the consumption rate rises, the system experiences qualitative alterations in stability: slightly increase of predation pressure may either mitigate the disease or, in adverse initial circumstances, precipitate predator extinction. Moderate consumption rate pushes the system into a multi-stable state, which shows how complicated predator–prey interactions can be, when there is moderate ecological stress. At a crucial threshold, the system undergoes a Hopf bifurcation, resulting in oscillatory dynamics around the disease-free state, characterised by fluctuations in prey and susceptible predator populations. For high consumption rate system only persist susceptible predator. We observed that lower amount of disease transmission supports to maintain disease free state. Moderate disease transmission rare leads to the system (1) in a bi-stsbility nature in between stable endemic and and disease free state. For high disease transmission rate protect the infected population from extinction which leads to the system (1) towards stable endemic state. In contrast our results partially align with the findings of [18] and [10], yet also revealed significant differences. Specifically, under low disease transmission rates leading to the extinction of infected predator our findings consistent with their conclusion. As disease transmission rate increases, our result agreed with the previous studies

in showing a rise in infected predator population accompanied by barely decline in susceptible predator. However, unlike [18] our study illustrates that at elevated transmission rates, the prey population can endure, primarily due to the decline of the vulnerable predator population. Furthermore our observation differ notably from those of [10] while they stated an unstable nature at moderate amount of transmission rate but our findings suggested that bi-stable nature in between stable disease free and endemic nature depends on the initial condition. Along with that the treatment effect showed the bi-stability nature for moderate value in between $E_3$ and $E^*$ depending on initial condition. Low treatment rate helps to persist the infected predator in the proposed system (1) and high treatment leads to the system (1) disease free stable state. Our finding partially align with the Mondal et al. [10] observations for low and high value of treatment. Differ for moderate amount of treatment, our findings suggested bi-stability but [10] observed oscillatory nature. In addition, to study the effect on system (1) simultaneously varying two parameters, we consider two parameter bifurcations (see Figs. 21, 22, 23, 24) to know the state of stability as well as instability and contour diagram (see Fig. 20) to judge the density of the species.

We also determine the global behavior analytical conditions and established the result with the help of numerical simulation. Considering the parametric values from the Table 1 for stable unique equilibrium state with different initial conditions (see Fig. 25). Also the system (1) globally stable around equilibria $E_3$ and $E_2$ for the parametric value $\beta = 0.2$ and $f = 1.5$, other parameter values taken from Table 1 (see Figs. 26 and 27). Furthermore our optimal control replicated that treatment strategy has very effective for reducing the infected predator population and extensively removed from the system. Our numerical findings indicate that system (1) exhibits multiple dynamical states depending on the parametric values. The system (1) demonstrates bi-stability and multi-stability for particular parameter regimes, where the converges equilibrium depends on initial species size. In addition, the system (1) attains global stability around the equilibrium points $E^*$, $E_3$ and $E_2$ for three distinct sets of parameter values, which are separate from those exhibiting bi-stability or multi stability. The presence of refuge able to protect the prey species in the proposed system (1) up to a stipulated amount of fear induced by the susceptible predator, which quite significant in ecological point on view. Furthermore susceptible predator able to sustain in every situation for the experimented parametric values from Table 1, because of modified Leslie-Gower model specifically we can say that presence of alternating food resources protect them from extinction. It's observed that infected predator eradicate from the system whenever the susceptible predator biomass decline and shortage of prey population due to the infected predator biomass totally depends on transmission from susceptible predator and sustain on the prey food. Lastly induction of treatment play a crucial role in the system dynamics, high treatment rate easily protect the system from infection which established through optimal control. So our analytical and numerical results reveal that larger refuge size and stronger treatment effects effectively reduce disease prevalence. Though fear on prey species control by refuge. Moreover the model exhibits parameter dependent bi-stability, multi-stability and global stability.

**Acknowledgements** The authors extend their heartfelt appreciation to the reviewers for their invaluable comments and insightful suggestions, which significantly enhanced and refined this paper.

**Author contributions** RK: Conceptualization, Methodology, Investigation, Analysis, Write the Main Manuscript. SB: Conceptualization, Methodology, Investigation, Analysis, Write the Main Manuscript. AKP: Conceptualization, Methodology, Investigation, Analysis, Write the Main Manuscript. JJN: Reviewing, Editing, Writing, Resources, Review & Editing, Supervision, Project Administration.

**Funding** Open Access funding provided thanks to the CRUE-CSIC agreement with Springer Nature. J. J. Nieto was supported by Agencia Estatal de Investigación of Spain Grant PID2020–113275GB-I00 funded by MCIN/AEI/10.13039/501,100,011,033 and by "ERDF A way of making Europe", "European Union" and Xunta de Galicia, grant ED431C 2023/12 for Competitive Reference Research Groups (2023–2026).

**Data availability** No datasets were generated or analysed during the current study.

## Declarations

**Conflict of interest** The authors declare no Conflict of interest.



## References

1. Das, A., Sahoo, D., Samanta, G., Nieto, J.J.: Deterministic and stochastic analysis of a two-prey–one-predator system with fear effect and switching behaviour in predation. Int. J. Dyn. Control **11**(3), 1076–1101 (2023). https://doi.org/10.1007/s40435-022-01028-x
2. Sardar, M., Khajanchi, S., Biswas, S.: Stochastic dynamics of a nonlinear tumor-immune competitive system. Nonlinear Dyn. **113**(5), 4395–4423 (2025). https://doi.org/10.1007/s11071-024-09768-5

3. Zhai, S., Tang, Y., Ma, J., Tao, J.: The role of fear and public opinion in mitigating the impact of deniers during epidemics. Chaos, Solitons & Fractals **199**, 116622 (2025). https://doi.org/10.1016/j.chaos.2025.116622
4. Kar, R., Biswas, S., Pal, A.K., Tiwari, P.K.: Dynamics of an eco-epidemiological model with mutual interference and nonlinear harvesting of predator. J. Appl. Math. Comput. **71**(3), 4095–4120 (2025). https://doi.org/10.1007/s12190-025-02384-5
5. Thirthar, A.A., Naji, R.K., Bozkurt, F., Yousef, A.: Modeling and analysis of an SI1I2R epidemic model with nonlinear incidence and general recovery functions of I1. Chaos, Solitons & Fractals **145**, 110746 (2021). https://doi.org/10.1016/j.chaos.2021.110746
6. Malthus, T.: An essay on the principle of population, as it affects the future improvement of society, with remarks on the speculations of Mr. Godwin, M. Condorcet, and other writers. In Charity and Philanthropy in Nineteenth-Century Britain (pp. 5-7). Routledge (1798)
7. Lotka, A.J.: Elements of physical biology. Williams and Wilkins (1925)
8. Volterra, V.: Variazioni e fluttuazioni del numero d'individui in specie animali conviventi. Società anonima tipografica" Leonardo da Vinci" (1926)
9. Jamil, A.R.M., Naji, R.K.: Modeling and analysis of the influence of fear on the harvested modified Leslie-Gower model involving nonlinear prey refuge. Mathematics. **10**, 2857 (2022). https://doi.org/10.3390/math10162857
10. Mondal, B., Sarkar, A., Sk, N.: Treatment of infected predators under the influence of fear-induced refuge. Sci. Rep. **13**(1), 16623 (2023). https://doi.org/10.1038/s41598-023-43021-0
11. Anderson, R.M., May, R.M.: Regulation and stability of host-parasite population interactions. J. Anim. Ecol. **47**(1), 219–247 (1978)
12. Chattopadhyay, J., Arino, O.: A predator-prey model with disease in the prey. Nonlinear Anal. **36**, 747–766 (1999)
13. Greenhalgh, D., Haque, M.: A predator–prey model with disease in the prey species only. Math. Methods Appl. Sci. **30**(8), 911–929 (2007). https://doi.org/10.1002/mma.815
14. Jana, S., Kar, T.K.: Modeling and analysis of a prey–predator system with disease in the prey. Chaos, Solitons & Fractals **47**, 42–53 (2013). https://doi.org/10.1016/j.chaos.2012.12.002
15. Aziz, S.F., Ahmed, H.J., Fatah, S.M., Mustafa, A.N.: Local Bifurcation and Global Stability of an Eco-Epidemiological Model Incorporating Fear Effect and Prey Harvesting. Int. J. Math. Math. Sci. **2025**(1), 6662455 (2025). https://doi.org/10.1155/ijmm/6662455
16. Ibrahim, H.A., Naji, R.K.: A prey-predator model with Michael Mentence type of predator harvesting and infectious disease in prey. Iraqi J. Sci. **61**(1), 1146–1163 (2020). https://doi.org/10.24996/ijs.2020.61.5.23
17. Wang, M., Yao, S.: The dynamics of an eco-epidemiological prey–predator model with infectious diseases in prey. Commun. Nonlinear Sci. Numer. Simul. **132**, 107902 (2024). https://doi.org/10.1016/j.cnsns.2024.107902
18. Sha, A., Chattopadhyay, J.: Dynamical study of fear effect in prey–predator model with disease in predator. J. Biol. Syst. **31**(04), 1319–1340 (2023). https://doi.org/10.1142/S0218339023500444
19. Mondal, A., Pal, A.K., Samanta, G.P.: On the dynamics of evolutionary Leslie-Gower predator-prey eco-epidemiological model with disease in predator. Ecol. Genet. Genom. **10**, 100034 (2019). https://doi.org/10.1016/j.egg.2018.11.002
20. Pal, A.K.: Effect of fear on a modified Lesli-Gower predator-prey eco-epidemiological model with disease in predator. J. Appl. Math. Inform. **38**(5–6), 375–406 (2020). https://doi.org/10.14317/jami.2020.375
21. Biswas, S., Samanta, S., Chattopadhyay, J.: A cannibalistic eco-epidemiological model with disease in predator population. J. Appl. Math. Comput. **57**, 161–197 (2018). https://doi.org/10.1007/s12190-017-1100-9
22. Mekonen, K.G., Bezabih, A.F., Rao, K.P.: Mathematical Modeling of Infectious Disease and Prey-Predator Interaction with Optimal Control. Int. J. Math. Math. Sci. **2024**(1), 5444627 (2024). https://doi.org/10.1155/2024/5444627
23. Zhai, S., Zhang, J., Tang, Y., Ma, J.: Impact of human intervention and predator-prey dynamics on ecosystem virus transmission. Chaos Interdiscipl. J. Nonlinear Sci. **35**(1), 013146 (2025). https://doi.org/10.1063/5.0247884
24. Ripple, W.J., Beschta, R.L.: Wolves and the ecology of fear: can predation risk structure ecosystems? Bioscience **54**(8), 755–766 (2004). https://doi.org/10.1641/0006-3568(2004)054[0755:WATEOF]2.0.CO;2
25. Suraci, J.P., Clinchy, M., Dill, L.M., Roberts, D., Zanette, L.Y.: Fear of large carnivores causes a trophic cascade. Nat. Commun. **7**(1), 10698 (2016). https://doi.org/10.1038/ncomms10698
26. Hua, F., Sieving, K.E., Fletcher, R.J., Jr., Wright, C.A.: Increased perception of predation risk to adults and offspring alters avian reproductive strategy and performance. Behav. Ecol. **25**(3), 509–519 (2014). https://doi.org/10.1093/beheco/aru017
27. Wang, X., Zanette, L., Zou, X.: Modelling the fear effect in predator–prey interactions. J. Math. Biol. **73**(5), 1179–1204 (2016). https://doi.org/10.1007/s00285-016-0989-1
28. Wang, X., Zou, X.: Modeling the fear effect in predator–prey interactions with adaptive avoidance of predators. Bull. Math. Biol. **79**, 1325–1359 (2017). https://doi.org/10.1007/s11538-017-0287-0
29. Zanette, L.Y., White, A.F., Allen, M.C., Clinchy, M.: Perceived predation risk reduces the number of offspring songbirds produce per year. Science **334**(6061), 1398–1401 (2011). https://doi.org/10.1126/science.1210908
30. Barman, D., Roy, J., Alrabaiah, H., Panja, P., Mondal, S.P., Alam, S.: Impact of predator incited fear and prey refuge in a fractional order prey predator model. Chaos, Solitons Fractals **142**, 110420 (2021). https://doi.org/10.1016/j.chaos.2020.110420
31. Chen, M., Takeuchi, Y., Zhang, J.F.: Dynamic complexity of a modified Leslie-Gower predator–prey system with fear effect. Commun. Nonlinear Sci. Numer. Simul. **119**, 107109 (2023). https://doi.org/10.1016/j.cnsns.2023.107109
32. Sarkar, K., Khajanchi, S.: Impact of fear effect on the growth of prey in a predator-prey interaction model. Ecol. Complex. **42**, 100826 (2020). https://doi.org/10.1016/j.ecocom.2020.100826
33. Panday, P., Samanta, S., Pal, N., Chattopadhyay, J.: Delay induced multiple stability switch and chaos in a predator–prey model with fear effect. Math. Comput. Simul. **172**, 134–158 (2020). https://doi.org/10.1016/j.matcom.2019.12.015
34. Mandal, M., Jana, S., Nandi, S.K., Kar, T.K.: Modelling and control of a fractional-order epidemic model with fear effect. Energy, Ecol. Environ. **5**(6), 421–432 (2020). https://doi.org/10.1007/s40974-020-00192-0
35. Rosenzweig, M.L., MacArthur, R.H.: Graphical representation and stability conditions of predator-prey interactions. Am. Nat. **97**(895), 209–223 (1963). https://doi.org/10.1086/282272
36. Huang, Y., Chen, F., Zhong, L.: Stability analysis of a prey-predator model with Holling type III response function incorporating a prey refuge. Appl. Math. Comput. **182**(1), 672–683 (2006). https://doi.org/10.1016/j.amc.2006.04.030
37. Vinoth, S., Vadivel, R., Hu, N.T., Chen, C.S., Gunasekaran, N.: Bifurcation analysis in a harvested modified Leslie-Gower model incorporated with the fear factor and prey refuge. Mathematics **11**(14), 3118 (2023). https://doi.org/10.3390/math11143118
38. Sasmal, S.K.: Population dynamics with multiple Allee effects induced by fear factors–A mathematical study on prey-predator interactions. Appl. Math. Model. **64**, 1–14 (2018). https://doi.org/10.1016/j.apm.2018.07.021

39. Cresswell, W.: Predation in bird populations. J. Ornithol. **152**(Suppl 1), 251–263 (2011). https://doi.org/10.1007/s10336-010-0638-1
40. Leslie, P.H.: Some further notes on the use of matrices in population mathematics. Biometrika **35**(3/4), 213–245 (1948). https://doi.org/10.2307/2332342
41. Leslie, P.H., Gower, J.C.: The properties of a stochastic model for the predator-prey type of interaction between two species. Biometrika **47**(3/4), 219–234 (1960). https://doi.org/10.2307/2333294
42. Aziz-Alaoui, M.A., Okiye, M.D.: Boundedness and global stability for a predator-prey model with modified Leslie-Gower and Holling-type II schemes. Appl. Math. Lett. **16**(7), 1069–1075 (2003). https://doi.org/10.1016/S0893-9659(03)90096-6
43. Roy, S., Tiwari, P.K., Nayak, H., Martcheva, M.: Effects of fear, refuge and hunting cooperation in a seasonally forced eco-epidemic model with selective predation. Eur. Phys. J. Plus **137**(5), 528 (2022). https://doi.org/10.1140/epjp/s13360-022-02751-2
44. Sk, N., Pal, S.: Dynamics of an infected prey–generalist predator system with the effects of fear, refuge and harvesting: Deterministic and stochastic approach. Eur. Phys. J. Plus **137**(1), 138 (2022). https://doi.org/10.1140/epjp/s13360-022-02348-9
45. Wobeser, G.: Disease management strategies for wildlife. Revue Scientifi. Tech. (Int. Office Epizootics) **21**(1), 159–178 (2002). https://doi.org/10.20506/rst.21.1.1326
46. Rowe, M.L., Whiteley, P.L., Carver, S.: The treatment of sarcoptic mange in wildlife: a systematic review. Parasit. Vect. **12**(1), 99 (2019). https://doi.org/10.1186/s13071-019-3340-z
47. El-Shahed, M., Moustafa, M.: Dynamics of a Fractional-Order Eco-Epidemiological Model with Two Disease Strains in a Predator Population Incorporating Harvesting. Axioms (2075-1680) **14**(1), 53 (2025). https://doi.org/10.3390/axioms14010053
48. Sotomayor, J.: Generic bifurcations of dynamical systems. In Dynamical systems (pp. 561-582). Academic Press. https://doi.org/10.1016/B978-0-12-550350-1.50047-3 (1973)